UNIVERSIDADE
BEIRA INTERIOR

Formulation and characterization of taxifolin delivery systems as an anti-Human Papillomavirus drug

Versão final após defesa

Miguel Leite Neto

Dissertação para obtenção do Grau de Mestre em
Ciências Biomédicas
(2º ciclo de estudos)

Orientador: Prof.ª Doutora Ângela Maria Almeida de Sousa
Coorientador: Prof.ª Doutora Diana Rita Barata Costa

novembro 2023

Declaração de Integridade

Eu, Miguel Leite Neto, que abaixo assino, estudante com o número de inscrição M11494 de Ciências Biomédicas da Faculdade Ciências da Saúde, declaro ter desenvolvido o presente trabalho e elaborado o presente texto em total consonância com o **Código de Integridades da Universidade da Beira Interior**.

Mais concretamente afirmo não ter incorrido em qualquer das variedades de Fraude Académica, e que aqui declaro conhecer, que em particular atendi à exigida referenciação de frases, extratos, imagens e outras formas de trabalho intelectual, e assumindo assim na íntegra as responsabilidades da autoria.

Universidade da Beira Interior, Covilhã 23 /11 /2023

Assinado por: **Miguel Leite Neto**
Num. de Identificação: 30128062
Data: 2023.11.23 21:27:40+00'00'

(assinatura conforme Cartão de Cidadão ou preferencialmente
assinatura digital no documento original se naquele mesmo formato)

Acknowledgments

I would like to express my heartfelt gratitude to all those who have contributed to the completion of my dissertation. This journey has been a challenging yet immensely rewarding endeavour, and I could not have reached this milestone without the support and encouragement of many whom I particularly thank.

First and foremost, I want to extend my deepest appreciation to my dissertation advisors, professor doctor Ângela Sousa and professor doctor Diana Costa for the opportunity you gave me to join your amazing work group and for all the guidance, expertise and unwavering belief in my abilities throughout this entire process. Their mentorship has not only shaped my research but has also enriched my academic and personal growth. I also thank professor doctor Luís Passarinha for all support and guidance provided in HPLC experiments.

I thank the University of Beira Interior, especially the Health Sciences Research Centre, for the facilities, equipment's and available material.

I would like to acknowledge the immense assistance of my fellow graduate students and research colleagues. Your friendship, shared experiences and intellectual exchange have been a source of inspiration. My deepest and special thanks to Miguel Ferreira and Diana Gomes for helping and supporting me along this process, teaching me techniques applied in this work as well as debating and assisting in all experiments and also to foster a culture of critical and innovative thinking.

To all my friends who have walked with me all along this path, my sincere thanks for all patience, understanding and friendship.

Last but definitely not least, a huge thanks to my family for the transmitted unshakable strength, patience, support, understanding and encouragement during this journey. To my parents, thank you for all the efforts, dedication, love and support. You have really been a pillar of strength and motivation.

This dissertation represents the culmination of years of hard work and dedication, and I am happy to share this achievement with all of you.

Resumo alargado

O cancro representa uma das principais causas de mortalidade em todo o mundo, registando mais de 19,3 milhões de casos em 2020, resultando em aproximadamente 10 milhões de mortes. Diversos fatores de risco já foram associados ao desenvolvimento de cancro, incluindo predisposição genética, estilos de vida, infeções provocadas por bactérias, parasitas ou vírus, etnia, exposição ambiental e idade-

O vírus do papiloma humano (HPV) é o principal agente causador de cancro do colo do útero, que, por sua vez, é o quarto cancro mais comum em mulheres em todo o mundo e responsável por mais de 340.000 mortes, apenas em 2020. Este tipo de cancro caracteriza-se pela excessiva expressão das oncoproteínas E6 e E7, que alteram a regulação do ciclo celular e a sua proliferação, comprometendo as funções das proteínas supressoras de tumores p53 e pRb, respetivamente.

Encontram-se disponíveis vacinas preventivas anti-HPV, no entanto, a sua administração não é globalmente realizada. Consequentemente, permanecem em andamento esforços para o desenvolvimento de terapias eficazes destinadas para este tipo de cancro com o objetivo de se obter uma cura eficaz. Neste sentido, os flavonoides têm demonstrado um notável potencial terapêutico, oferecendo uma abordagem acessível e eficaz, permitindo a sua utilização em países em desenvolvimento e onde, geralmente, os cuidados de saúde são muito limitados.

A taxifolina é um flavonoide com várias propriedades anticancerígenas, já tendo mostrado particular relevância na terapia do cancro do colo do útero devido ao facto de potenciar a inibição da oncoproteína E6, fazendo assim com que haja um aumento da expressão da p53, induzindo apoptose. Contudo, o uso da taxifolina é limitado devido à sua baixa solubilidade aquosa e baixa estabilidade. Por conseguinte, a sua fraca biodisponibilidade limita as suas aplicações em terapias do cancro.

Desta forma, esta dissertação de mestrado tem por objetivo desenvolver sistemas de entrega para a encapsulação eficiente de taxifolina visando melhorar a sua biodisponibilidade e efeito em células HPV positivas.

Para isso, foram desenvolvidos vários sistemas de entrega, constituídos por quitosano, gelana e taxifolina. Primeiramente, foram testados vários rácios de sistemas formulados apenas com quitosano de baixo peso molecular e gelana. O rácio mais favorável apresentou um tamanho de 238,07 ± 31,18 nm, um PdI de 0,29 ± 0,08 e um potencial zeta de +22,56 ± 2,83 mV e foi o escolhido para prosseguir com os estudos e tentar a encapsulação de taxifolina. Para a incorporação de taxifolina nos sistemas de entrega, foram

testados vários tipos de quitosano (5 kDa, baixo peso molecular e alto peso molecular) em vários rácios de taxifolina. Os sistemas constituídos por quitosano de baixo peso molecular (LMW CH/GG/TAX) apresentaram um tamanho de 276,23 ± 30,68, um PdI de 0,36 ± 0,06 e um potencial zeta de +30,80 ± 5,66 mV. Por sua vez, os sistemas de entrega formados por quitosano de alto peso molecular (HMW CH/GG/TAX) mostraram um tamanho de 272,82 ± 53,58 nm, um PdI de 0,33 ± 0,10 e um potencial zeta de +23,59 ± 5,94 mV, enquanto os sistemas compostos por quitosano de 5 kDa (5 kDa CH/GG/TAX) apresentaram um tamanho de 249,00 ± 12,58 nm, um PdI de 0,35 ± 0,10 e um potencial zeta de +17,35 ± 5,64 mV. Relativamente à eficiência de encapsulação de taxifolina, os sistemas LMW CH/GG/TAX apresentaram uma eficiência de 65% enquanto os restantes sistemas apenas encapsularam 55%.

Foi ainda realizada microscopia eletrónica de varrimento (SEM) às amostras dos sistemas formulados e foi possível verificar que todos os sistemas apresentaram forma esférica e uniforme. Além disso, foi também realizada espetroscopia de infravermelho por transformada de Fourier (FTIR) e espetroscopia de UV/vis para verificar a presença e interações dos compostos presentes nos sistemas de entrega.

Por fim, foram realizados ensaios de libertação *in vitro* a 2 pHs diferentes, um representativo do microambiente tumoral (pH 5.8) e um representativo do pH fisiológico (pH 7.4). Os resultados mostraram que os sistemas HMW CH/GG/TAX libertaram cerca de 45% e 80% de taxifolina a pH 5.8 e pH 7.4, respetivamente. Os sistemas LMW CH/GG/TAX libertaram 25% a pH 7.4 e cerca de 70% a pH 5.8. Os sistemas 5 kDa CH/GG/TAX libertaram entre 20% e 40% nos 2 diferentes pHs.

Com base em toda a informação obtida sobre a caracterização dos sistemas de entrega, apenas o mais favorável, a formulação LMW CH/GG/TAX, prosseguiu para ensaios celulares, onde foi realizado ensaio de internalização em células saudáveis e células HPV positivas. Os resultados demonstraram que os sistemas de entrega foram capazes de internalizar nas duas linhas celulares, no entanto, é expectável que taxifolina apenas tenha efeito nas células HPV positivas, devido à ação especifica contra a oncoproteína E6.

Palavras-chave

Cancro do colo do útero;flavonoides;HPV;sistemas de entrega;taxifolina

Abstract

Cancer is a leading cause of mortality worldwide, with over 19.3 million cases reported in 2020, resulting in approximately 10 million deaths. Various risk factors have been associated with the development of cancer, including age, genetic predisposition, ethnicity, environmental exposure, lifestyle, and infections caused by bacteria, parasites, or viruses.

Human papillomavirus (HPV) is the primary causative agent of cervical cancer, which is the fourth most common cancer in women worldwide, responsible for over 340,000 deaths in 2020. This cancer is characterized by the overexpression of oncoproteins E6 and E7, which disrupt cell cycle regulation and proliferation, compromising the functions of tumor suppressor proteins p53 and pRb, respectively.

Despite the availability of preventive HPV vaccines, their administration is not universally carried out. Consequently, efforts continue to develop effective therapies for this type of cancer to achieve a successful cure. In this regard, flavonoids have demonstrated remarkable therapeutic potential, offering an accessible and effective approach, allowing their use in less developed countries with limited healthcare resources.

Taxifolin is a flavonoid with several anticancer properties, having shown particular relevance in cervical cancer therapy due to its ability to enhance the inhibition of oncoprotein E6, thereby increasing p53 expression and inducing apoptosis. However, the use of taxifolin is limited due to its very low aqueous solubility and low stability. Consequently, its poor bioavailability restricts its applications in cancer therapies.

Thus, this master's dissertation aims to develop delivery systems for the encapsulation of taxifolin to improve its bioavailability and effectiveness in HPV-positive cells. To achieve this, various delivery systems consisting of chitosan, gelatin, and taxifolin were formulated. Initially, several ratios of systems composed solely of low molecular weight chitosan and gellan gum were tested. The most favourable ratio exhibited a size of 238.07 ± 31.18 nm, a PdI of 0.29 ± 0.08, and a zeta potential of +22.56 ± 2.83 mV and was chosen to proceed with the studies and attempt taxifolin encapsulation.

For the incorporation of taxifolin into the delivery systems, various types of chitosan (5 kDa, low molecular weight, and high molecular weight) were tested at various taxifolin ratios. Systems composed of low molecular weight chitosan (LMW CH/GG/TAX) had a size of 276.23 ± 30.68 nm, a PdI of 0.36 ± 0.06, and a zeta potential of +30.80 ± 5.66 mV. Delivery systems formed by high molecular weight chitosan (HMW CH/GG/TAX) showed a

size of 272.82 ± 53.58 nm, a PdI of 0.33 ± 0.10, and a zeta potential of +23.59 ± 5.94 mV, while systems composed of 5 kDa chitosan (5 kDa CH/GG/TAX) had a size of 249.00 ± 12.58 nm, a PdI of 0.35 ± 0.10, and a zeta potential of +17.35 ± 5.64 mV. Regarding encapsulation efficiency, LMW CH/GG/TAX exhibited an efficiency of 65%, while the remaining systems encapsulated only 55%.

Scanning electron microscopy (SEM) was also performed for all formulated samples, and it was possible to observe that all systems exhibited a spherical and uniform morphology. In addition, Fourier-transform infrared spectroscopy (FTIR) and UV/vis spectroscopy were conducted to verify the presence and interactions of compounds in the delivery systems.

Finally, *in vitro* release assays were performed at two different pH levels, one representative of the tumor microenvironment (pH 5.8) and one representative of physiological pH (pH 7.4). The results showed that HMW CH/GG/TAX systems released approximately 45% and 80% of taxifolin at pH 5.8 and pH 7.4, respectively. LMW CH/GG/TAX systems released 25% at pH 7.4 and approximately 70% at pH 5.8. The 5 kDa CH/GG/TAX systems released between 20% and 40% at the two different pH levels.

Based on all the gathered information regarding the characterization of the delivery systems, only the most favourable formulation, LMW CH/GG/TAX, proceeded to cellular assays, where internalization assays were conducted on healthy cells and HPV-positive cells. The results demonstrated that the delivery systems were capable of internalizing into both cell lines; however, it is expected that they will solely exert an effect on HPV-positive cells due to their specific action against oncoprotein E6.

Keywords

Cervical cancer;delivery systems;flavonoids;HPV;taxifolin

Index

1. Introduction 1

1.1. Cancer 1

1.2. Cervical Cancer 2

1.3. Human Papilloma Virus 4

1.4. HPV genome and life cycle 5

1.5. HPV E6 and E7 oncoproteins activities during the replication cycle 8

1.6. Current therapies 10

1.7. Flavonoids 11

1.8. Flavonoids subgroups 13

1.9. Flavones 14

1.10. Flavonols 15

1.11. Flavanones 15

1.12. Flavanols (Flavan-3-ols) 15

1.13. Isoflavonoids 16

1.14. Chalcones 16

1.15. Anthocyanidins 17

1.16. Flavonoids limitations 17

1.17. Delivery systems 17

1.18. Lipid based delivery systems 18

1.19. Liposomes 18

1.20. Emulsions and nanoemulsions 19

1.21. Lipid based nanoparticles 20

1.22. Polymer based nanoparticles 20

1.23. Natural polymers 21

1.24. Synthetic polymers 21

1.25. Inorganic polymers 22

1.26. Micelles 22

1.27. Inclusion complexes 23
1.28. Other types of delivery systems 24
1.29. Chitosan 24
1.30. Chitosan-based formulation methods 26
1.31. Ionic cross-linking 26
1.32. Precipitation or flocculation 27
1.33. Solvent evaporation 27
1.34. Spray drying 27
1.35. Chitosan coating solution 27
1.36. Polyelectrolyte complexation 27
1.37. Gellan gum 28
1.38. Taxifolin 29
2. Objectives 32
3. Materials and methods 34
3.1. Materials 34
3.2. Methods - Preparation of solutions 34
3.3. Preparation of chitosan and gellan gum systems 34
3.4. Preparation of taxifolin delivery systems 35
3.5. Nanoparticle size and zeta potential analysis 35
3.6. UV/vis Absorbance Spectrum 35
3.7. Scanning electron microscopy 35
3.8. Fourier-transform infrared spectroscopy 36
3.9. Encapsulation efficiency 36
3.10. *In vitro* release studies 37
3.11. Cell culture 38
3.12. Cell internalization 38
4. Results and discussion 40
4.1. Development of chitosan and gellan gum systems 40
4.2. UV/vis spectrum of CH/GG systems 42

4.3. Development of taxifolin delivery systems....43
4.4. Fourier transformed infrared spectroscopy....44
4.5. Different chitosan types....45
4.6. Scanning electron microscopy....46
4.7. Encapsulation efficiency....47
4.8. *In vitro* release studies....47
4.9. Delivery systems internalization studies....49
5. Conclusions and future perspectives....53
References....56

List of Figures

Figure 1 - Estimated cancer rate incidence in 2020, World, both sexes, all ages. 1
Figure 2 - Estimated cancer rate mortality in 2020, World, both sexes, all ages. 2
Figure 3 - Estimated cancer incidence rate, World, females, all ages..... 3
Figure 4 - Estimated cancer mortality rate, World, females, all ages. 3
Figure 5 - Estimated cancer incidence rate, Low Income Countries, females, all ages. 4
Figure 6 - Estimated cancer mortality rate, Low Income Countries, females, all ages.. 4
Figure 7 -Human Papilloma Virus genome structure. 6
Figure 8 - Schematic representation of HPV-infected squamous epithelial cells in normal, precancerous lesions and cancerous conditions. 8
Figure 9 - Synergetic effect of the HPV E6 and E7 oncoproteins. 10
Figure 10 - Basic chemical structure of flavonoids. 11
Figure 11 - Apoptotic pathways mediated by flavonoids..... 13
Figure 12 - Flavonoids classification: (**A**) flavones, (**B**) flavonols, (**C**) flavanones, (**D**) isoflavonoids, (**E**) flavanols, (**F**) chalcones, (**G**) anthocyanidins. 14
Figure 13 - Foremost types of delivery systems currently under development for the encapsulation of flavonoid. 18
Figure 14 - Chemical structure of chitosan. 25
Figure 15 - Chemical structure of gellan gum. 29
Figure 16 - Chemical structure of taxifolin. 30
Figure 17 - HPLC calibration curve for taxifolin in water. 37
Figure 18 - Size and PdI comparison between the same formulation in different flow rates. 41
Figure 19 - UV/vis spectrum of CH/GG systems. 42
Figure 20 – FTIR spectra of gellan gum, LMW Chitosan, CH/GG systems and CH/GG/TAX systems. 44
Figure 21 - SEM images: (**A**) CH/GG systems, (**B**) 5 kDa CH/GG/TAX systems, (**C**) LMW CH/GG/TAX, (**D**), HMW CH/GG/TAX systems. 46
Figure 22 - *In vitro* release studies: (**A**) pH 7.4, (**B**) pH 5.8. 48
Figure 23 - Uptake of FITC labelled LMW CH/GG/TAX delivery systems in HeLa cells: (**A**) control group (non-treated), (**B**) after 2 h of incubation, (**C**) after 4 h of incubation, (**D**) after 6 h of incubation. 49

Figure 24 - Uptake of FITC labelled LMW CH/GG/TAX delivery systems in hFiB cells: (**A**) control group (non-treated), (**B**) after 2 h of incubation, (**C**) after 4 h of incubation, (**D**) after 6 h of incubation. 50

List of Tables

Table 1 - HPV subgroups and associated diseases. 5
Table 2- HPV genotypes classification according to oncogenic potential. 5
Table 3- Major roles of proteins expressed by high-risk HPV. 6
Table 4- Current vaccines against HPV. 10
Table 5- Preparation conditions, mean size, PdI and zeta potential of CH/GG systems. 41
Table 6- Physico-chemical characterization of CH/GG/TAX formulations obtained by varying the volume of taxifolin solution dissolved in ethanol and water. 43
Table 7 - Size and Potential Zeta of nanoparticles with different types of chitosan. 45
Table 8 - Encapsulation efficiency of each delivery system. 47

List of abbreviations

CIS	Carcinoma in situ
CIN	Cervical intraepithelial neoplasia
DLS	Dynamic Light Scattering
DMEM F-12	Dulbecco's Modified Eagle's Medium/Ham's F-12 nutrient mixture
DMSO	Dimethyl sulfoxide
DNA	Deoxyribonucleic acid
E	Early region
E6AP	E6 associated-protein
EE	Encapsulation efficiency
FTIR	Fourier Transform infrared spectroscopy
GLOBOCAN	Global Cancer Observatory
HGCIN	High-grade cervical intraepithelial neoplasia
HMW	High molecular weight
HPLC	High-performance liquid chromatography
HPV	Human Papilloma Virus
L	Late region
LCR	Late control region
LGCIN	Low-grade cervical intraepithelial neoplasia
LMW	Low molecular weight
MTT	3-(4,5-dimethylthiazol-2-yl)-2,5-diphenyltetrazolium bromide
NLCs	Nanostructured lipid carriers
ORF	Open reading frames
PBS	Phosphate-buffered saline
PdI	Polydispersity Index
PEC	Polyelectrolyte complexes
PEG	Polyethylene glycol
pRb	Retinoblastoma protein
RNA	Ribonucleic acid
ROS	Reactive oxygen species
SEM	Scanning electron microscopy
SLNs	Solid Lipid nanoparticles

UV	Ultraviolet
ZP	Zeta Potential

List of Scientific Publications

Original paper: Ferreira, Miguel & Gomes, Diana & Neto, Miguel & Passarinha, Luís & Costa, Diana & Sousa, Ângela. (2023). Development and Characterization of Quercetin-Loaded Delivery Systems for Increasing Its Bioavailability in Cervical Cancer Cells. Pharmaceutics. 15. 936. 10.3390/pharmaceutics15030936. (Not directly related to the main topic of this dissertation).

List of Scientific Communication

Oral communication: Neto, M.; Ferreira, M.; Gomes, D; Passarinha, L.A; Costa, D; Sousa, Â; Formulation and characterization of taxifolin-loaded nanoparticles; 2023; XVIII International CICS-UBI Symposium, Covilhã, Portugal.

Poster communication: Ferreira, M; Gomes, D; Neto, M; Passarinha, L.A; Costa, D; Sousa, Â; pH responsive quercetin-loaded nanoparticles for cervical cancer therapy; 2023; XVIII International CICS-UBI Symposium, Covilhã, Portugal. (Not directly related to the main topic of this dissertation).

1. Introduction

1.1. Cancer

Cancer is a tremendous burden on society, as it is the leading cause of mortality worldwide, accounting for almost 10 million deaths and nearly 20 million new cancer cases in 2020[1]. This disease can develop from any organ or structure in the body and is made up of small cells that have lost their ability to trigger apoptosis. In general, cancer must be 1 cm in size or have 1 million cells in order to be detected. Cancer can be defined as the abnormal development of cells[2]. However, the conversion of a normal cell into a malignant cell, as well as the inability of the body's immune cells to recognize and eliminate newly generated cancer cells when they are just a few in number, can be key events in the creation of cancer[3].

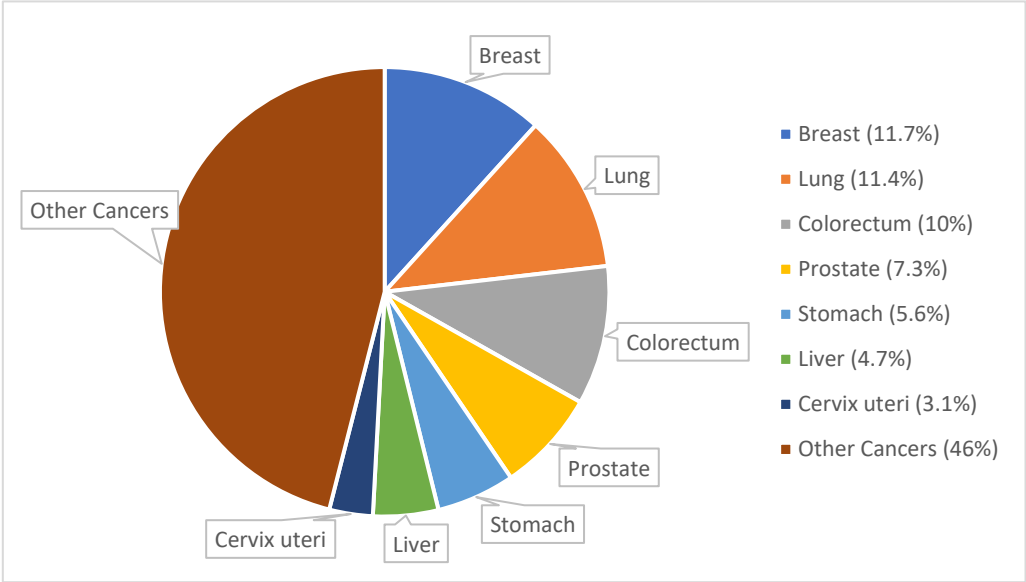

Figure 1 - Estimated cancer rate incidence in 2020, World, both sexes, all ages (adapted from[2]).

Globally, the most incident type of cancer is the breast cancer (11.7%), followed by lung cancer (11.4%) and colorectum cancer (10.0%), matching to almost a third of all cancers, as shown in Figure 1. Concerning the mortality rates, the lung cancer leads (18%), followed by colorectum (9.4%) and liver (8.3%) cancers[4], as displayed in Figure 2.

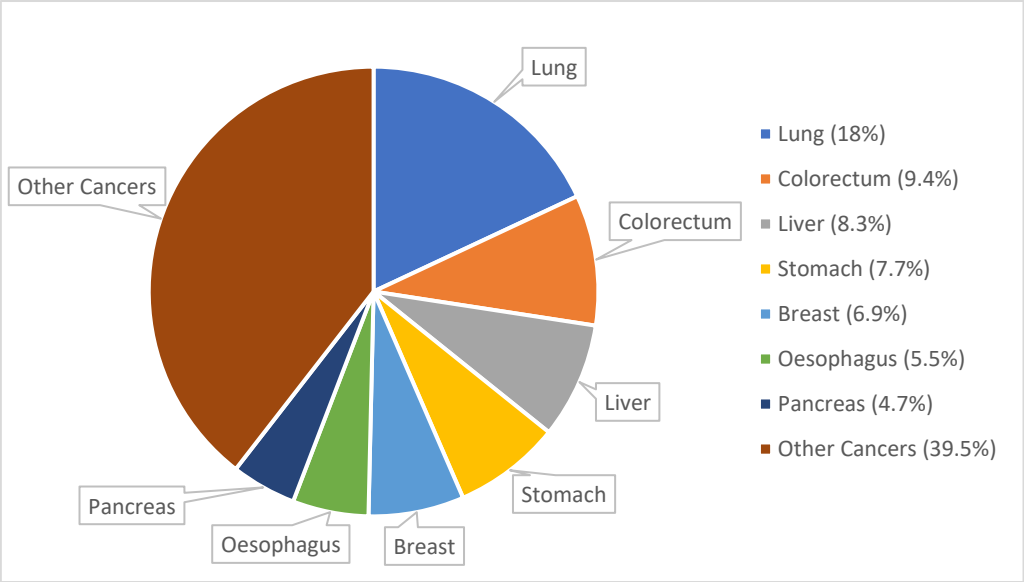

Figure 2 - Estimated cancer rate mortality in 2020, World, both sexes, all ages (adapted from[2]).

Unlike most diseases, cancer is not primarily caused by some foreign entity to our bodies. However, research has shown that are certain risk factors such as tobacco and alcohol usage, age, genetic predisposition, ethnicity, environmental exposure that may increase the risk of cancer development[5]. Nevertheless, there are other types of risk factors that are associated with cancer development, such as bacteria, parasites and viruses infections, such as the human papilloma virus (HPV), which distinguishes from others due to the high risk of develop cancers, like head, neck, vaginal, vulvar, penile, anal and particularly cervical cancer[6].

1.2. Cervical Cancer

Cervical cancer is the fourth most common cancer in women worldwide (6.5%), as shown in Figure 3, being highly associated with high-risk HPV subtypes.

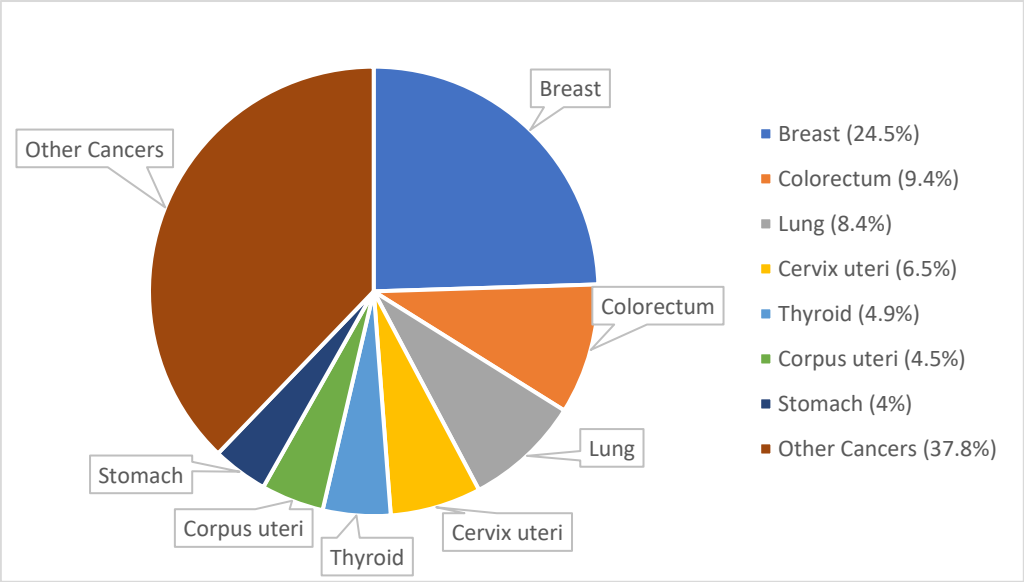

Figure 3 - Estimated cancer incidence rate, World, females, all ages (adapted from[2]).

Regarding the mortality rates, cervical cancer is also the fourth most common in women worldwide (7.7%), representing almost 350,000 deaths in 2020 alone, as Figure 4 points out.

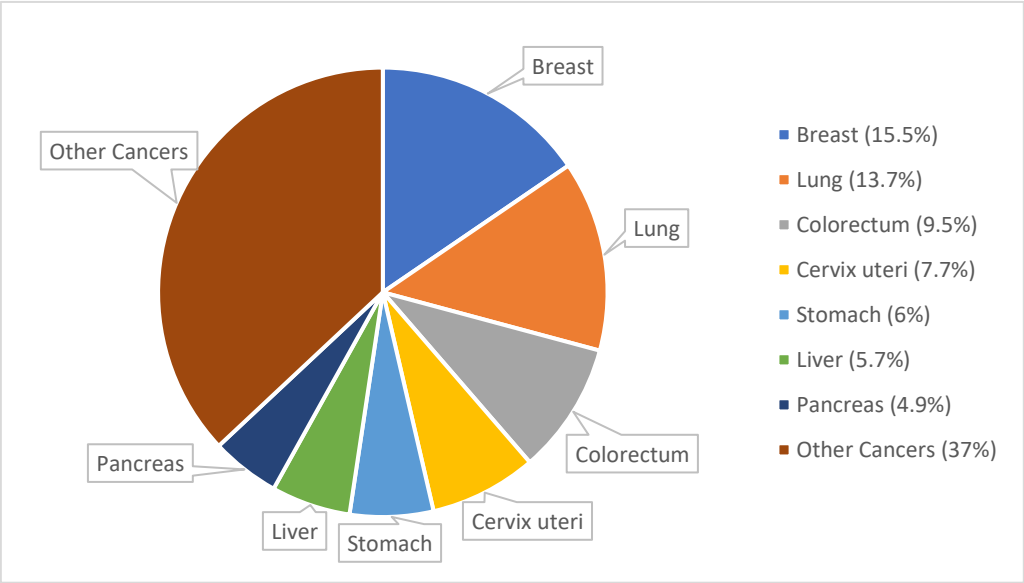

Figure 4 - Estimated cancer mortality rate, World, females, all ages (adapted from[2]).

Nonetheless, these figures are even more concerning in low-income countries, where cervical cancer is the second most common type of cancer and the second leading cause of death from cancer in women, with 17.9% and 18.9%, respectively, only being surpassed by breast cancer, as shown in Figures 5 and 6[7]. The human papillomavirus (HPV) is the primary cause of cervical cancer, accounting for 79% to 100% of

occurrences, with around 70% of cases associated with two high-risk subtypes, namely HPV 16 and HPV 18[8].

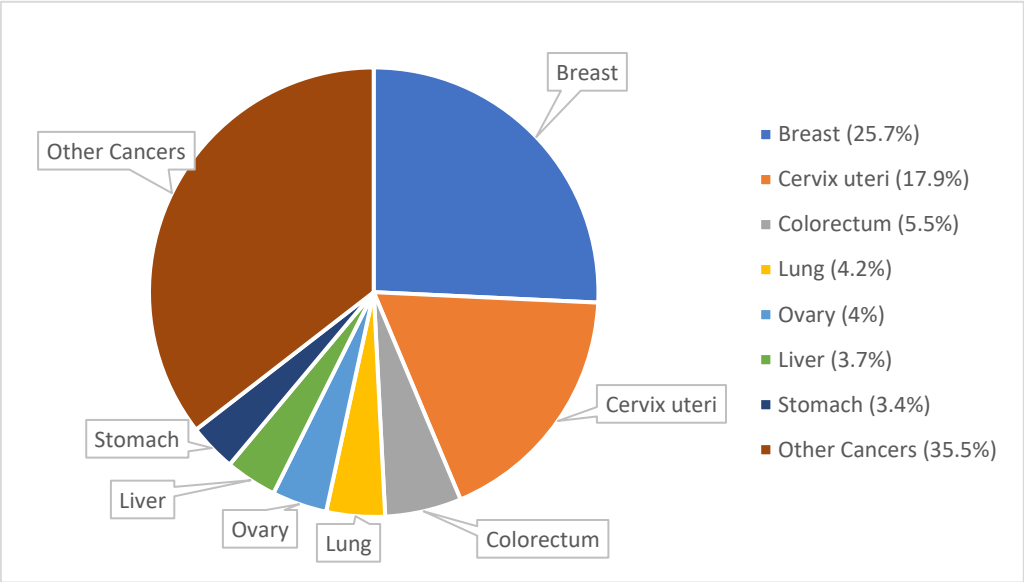

Figure 5 - Estimated cancer incidence rate, Low Income Countries, females, all ages. (adapted from[2]).

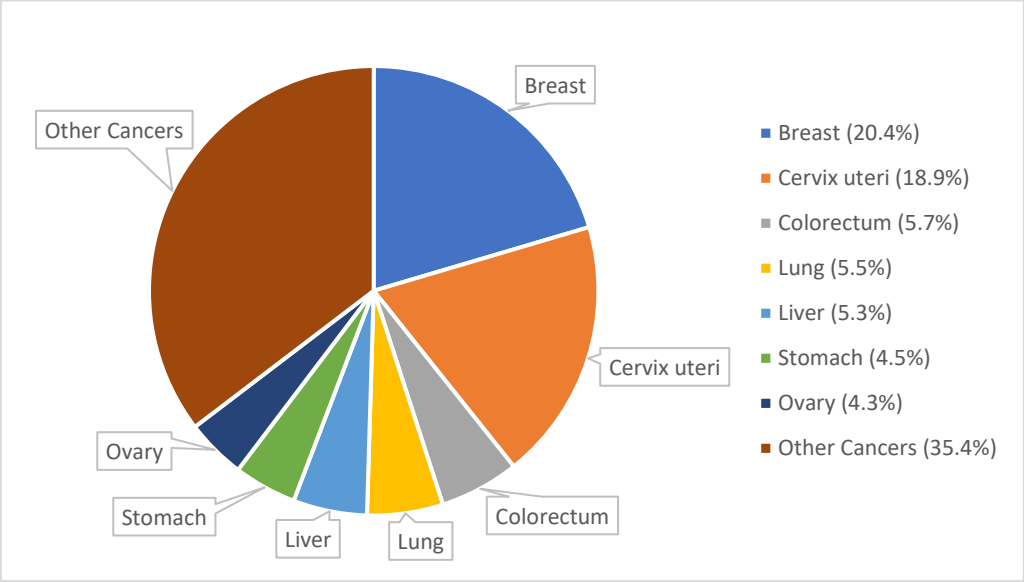

Figure 6 - Estimated cancer mortality rate, Low Income Countries, females, all ages. (adapted from[2]).

The discrepancy of the data between different regions of the world can be explained with the lack of healthcare and the network distribution of anti-HPV vaccines, which are way less in low-income countries.

1.3. Human Papilloma Virus

Human Papilloma Virus (HPV) is a common sexually transmitted infection that affects both men and women. It is estimated that up to 80% of all sexually active

individuals will contract HPV at some point in their lives[9]. As previously stated, HPV infections represent between 79 and 100% of all cervical cancers. HPV is spread through skin-to-skin contact during sexual activity, and it can be passed on even when the infected individual does not show any visible symptoms or signs of infection[10].

HPVs, also known as papillomaviruses, are capable to infect both cutaneous and mucosal epithelial cells and more than 200 different genotypes have been identified so far, which most of them typically cause benign conditions, such as warts or other lesions[11]. HPVs subgroups and their associated diseases are represented in Table 1.

Table 1 - HPV subgroups and associated diseases (adapted from[12]).

Subgroup	Epithelial Tropisms	Associated disease
Alpha	Mucosal and cutaneous	High-risk mucosal HPV types associated with cervical cancer. Low-risk mucosal and cutaneous HPV types that can cause benign lesions or skin warts.
Beta	Cutaneous	High-risk and low-risk HPV types associated with unapparent infections in immunocompromised hosts. Persistent infection may develop to skin cancer.
Gamma	Cutaneous	Benign cutaneous lesions. DNA very rarely found in skin cancers.
Mu	Cutaneous	Benign cutaneous lesions. Not associated with cancer.
Nu	Cutaneous	Benign cutaneous lesions. DNA only very rarely found in skin cancers.

Within the subgroup of *Alphapapillomaviruses*, the genotypes that infect the mucous membranes can also be classified in compliance to their oncogenic potential, being discriminated into low-risk and high-risk genotypes, as presented in Table 2[12].

Table 2- HPV genotypes classification according to oncogenic potential (adapted from[13]).

HPV classification	HPV genotype
Low-risk	6, 11, 40, 42, 43, 44, 54, 61, 70, 72 and 81
High-risk	16, 18, 31, 33, 35, 39, 45, 51, 52, 56, 58, 59, 68, 73 and 82

When it comes to their cancer-inducing ability, 15 are classified as high-risk HPV genotypes, being the HPV16 and HPV 18 the ones with the highest prevalence, accountable for 50 to 60% and 10 to 20% of all cervical cancer cases worldwide, respectively[13].

1.4. HPV genome and life cycle

HPVs are small viruses with a diameter of about 55 nm that have a non-enveloped icosahedral of approximately 8000 base pairs, circular structure, and a double-stranded DNA genome. This genome encodes 8 reading frames (ORF) and can be divided into three functional series, the early (E) region encoding at least seven proteins that have regulatory functions in the infected epithelial cell (E1,E2,E4,E5,E6,E7,E8), the late (L)

region that encodes the two viral structural proteins that form the viral capsid (L1 and L2) and the long control region (LCR), also known as upstream regulatory region (URR) that contain the viral *cis*-acting regulatory sequences that control viral replication and transcription, and post-transcription control via the LRE (late regulatory element)[14]. Figure 7 shows HPV genome structure and Table 3 display the major roles of proteins expressed by high-risk HPV.

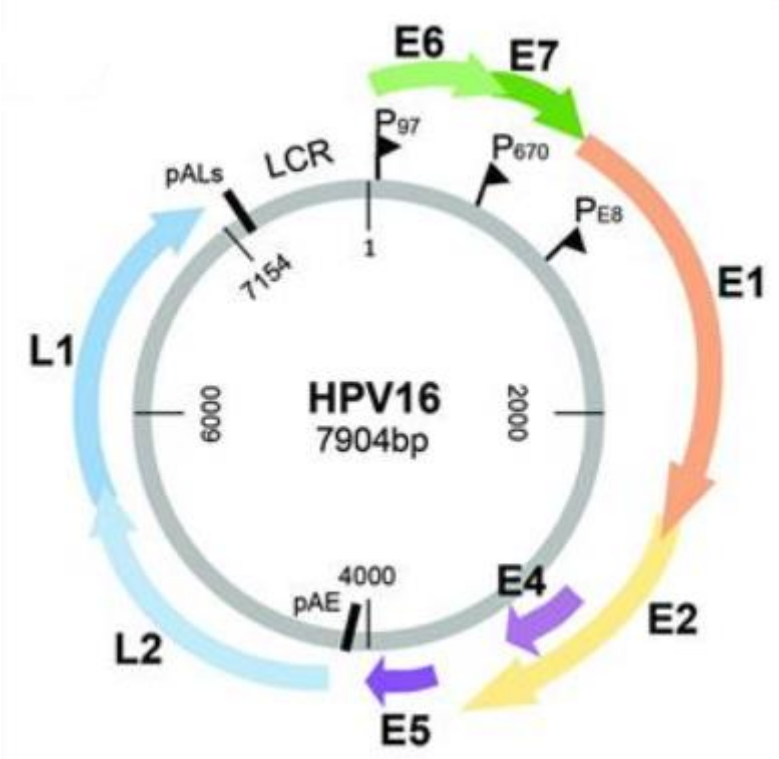

Figure 7 -Human Papilloma Virus genome structure (adapted from[16]).

Table 3- Major roles of proteins expressed by high-risk HPV (adapted from[15]).

Region	Protein	Role
Early	E1	Genome replication: ATP-dependent DNA helicase.
	E2	Viral DNA replication. E6 and E7 transcriptional repressor.
	E4	Cell cycle arrest. Virion assembly.
	E5	Control of cell growth and cell differentiation.
	E6	Oncoprotein. Induces degradation of p53. Regulates cell cycle.
	E7	Induces degradation of pRb. Cell cycle control.
Late	L1	Encodes major capsid protein (55 kDa).
	L2	Encodes minor capsid protein (70 kDa). Recruits L1.
Long control	LCR	Regulates viral replication and transcription.

The replication cycle of HPV is linked to differentiation of the epithelium that was infected[14]. HPV can entry into the epithelium through microabrasions or the HR-HPV strains invading the cervical epithelium via the cellular junction between the endo- and ectocervix[15]. The endocervical canal is lined with stratified squamous epithelium and

columnar epithelium that cover the ectocervix and endocervix, respectively, and the transition zone between these cells is called the squamocolumnar junction[16].

The HPV L1 capsid protein attaches to cellular receptors present on the basal membrane or the surface of basal layer cells. The initial binding of HPV seems to be facilitated by heparin sulphate proteoglycans (HSGPs), which appear to be the primary receptor. Such bond induces a conformational change in the viral capsid, mediated by cyclophilin B, leading to the exposure of the N-terminus of the L2 component on the surface of the virion.

After acquiring the infection, the early E1 and E2 proteins are expressed in the undifferentiated epithelial cells of the basal layer, thereby controlling viral replication and further expression of viral early proteins. At this juncture, the viral replication cycle is completely conditioned by the differentiation cycle of the infected cells, as the viral DNA replication only occurs when the DNA of the infected cells undergoes replication[17].

Viral proteins are probably expressed at low levels in infected basal cells to avoid activating the local immune response[18]. In this way, the HPV can continue to infect epithelial cells for a sizable amount of time. A transit amplifying cell can be created by the division of an infected basal epithelial cell. This cell differentiates and moves to the upper epithelial layers while carrying the viral genomes with it[19].

Hence, the infected basal cells, upon differentiation, will subsequently express E6 and E7 viral proteins. Both proteins serve as cell proliferation stimulators, prolong the progression of the cell cycle, and prevent apoptosis. The expression of these oncoproteins is a result of the absence of the E2 protein, which is no longer expressed after the integration of the DNA into the genome of infected cells. Because of E2 absence, an increased expression of E6 and E7 will occur, which further promotes the development of malignant lesions. During this stage, the infected cells exhibit an accelerated life cycle, dividing more frequently and leading to an increase in their population, gradually replacing normal cells[17]. The synthesis of L1 and L2 proteins occurs in the final phase of the cell cycle, primarily in the superficial layers of the epithelium[17]. Ultimately, the more differentiated cells produce virions that are released by keratinocytes situated in the outermost layers, as they die[17].

Figure 8 displays the distribution of epithelial cells in the normal cervix and HPV-infected cells in precancerous (CINs) and cancerous environment.

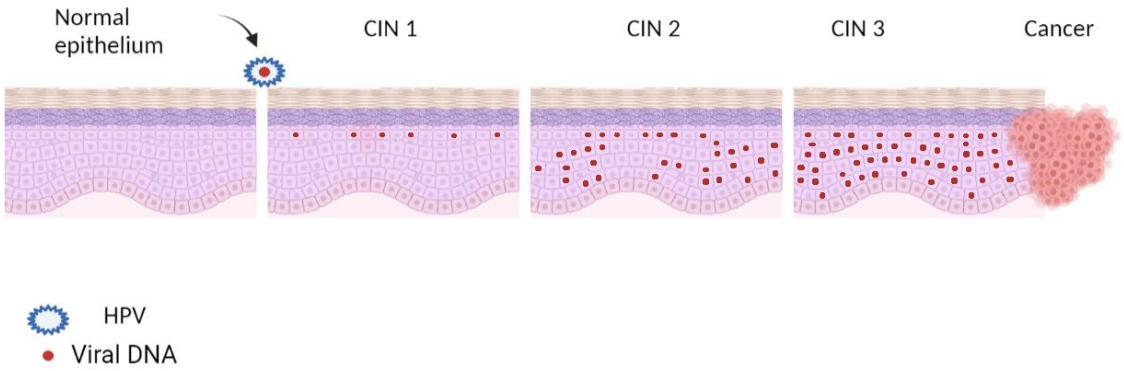

Figure 8 - Schematic representation of HPV-infected squamous epithelial cells in normal, precancerous lesions and cancerous conditions (adapted from[18]).

Carcinogenesis refers to the entire process from infection to the manifestation of cancer. As previously stated, any premalignant alteration of cells occurs mostly in the squamocolumnar junction and is strongly linked to HPV-16 and HPV-18. Cervical intraepithelial neoplasia (CIN) refers to these premalignant alterations or dysplasia of squamous cells in the cervical epithelium. If CIN is not treated early enough or if the HPV is able to deactivate the host cellular activities, it might develop to carcinoma in situ (CIS). The severity of CINs is classified histologically from 1 to 3. The epithelial cells are normally well structured. In CIN, CIS, and cancer, however, HPV-infected cells become dysplastic. CIN 1, also known as low-grade CIN (LGCIN), is a minor dysplasia characterized by abnormality of the lowest one-third of the epithelium. When two-thirds of the epithelium is affected, it is classified as CIN 2 or moderate dysplasia; when more than two-thirds of the epithelium is affected, it is classified as severe dysplasia or CIN 3. CIN 2 and CIN 3 lesions are both considered high-grade CIN (HGCIN)[16]. Figure 8 depicts the distribution of normal cervix epithelial cells and HPV-infected cells in precancerous (CINs) and cancerous environments.

1.5. HPV E6 and E7 oncoproteins activities during the replication cycle

Both E6 and E7 viral genes are present in the HPV genome and are transcribed in the infected cells, expressing their respective oncoproteins that emerge as the main oncogenic power.

The E7 oncoprotein consists of 98 amino acids and possesses a zinc-binding domain at its C-terminal that plays a crucial role in the activity of the oncoprotein[20]. Early in the infection, the expression of E7 triggers the activation of the G1 to S-phase checkpoint in keratinocytes that would typically undergo terminal differentiation. As a result, the compartment of epithelial cells that are activated in the DNA replication expands. E7 can activate the cycle of infected cells, differentiating them by binding and

releasing, or by degrading pRb and other pocket proteins (p107 and p130), from a transcriptional repression complex containing the E2F transcription factor. This combination inhibits cell proliferation by inhibiting the transcription of E2F-dependent genes. In the case of an HPV infection, the binding of E7 to pRb impairs the latter's capacity to control the E2F family transcription factors, resulting in continuous DNA replication and viral cycle progression[21].

In addition, during the viral life cycle, E7 is always present with E6 in the infected cells, probably due to the bicistronic nature of the E6/E7 coding region of the genome. Ergo, activities of either protein will be affected by the other and it is coherent that they often act co-operatively, for instance in avoiding immune detection[22].

Usually, cells respond to any kind of unscheduled event in cell proliferation by inducing apoptosis. So, it would be expected from cells to induce cell death due to E7 activity. In order to prevent this, HPVs express E6, an oncoprotein containing roughly 150-160 amino acids with a molecular weight of 18 kDa and four Cys-X-X-Cys motifs that generate two zinc fingers[23]. This oncoprotein binds to the E6-associated protein (E6AP), a ubiquitin ligase that is needed for p53 interaction. As a result of the creation of this trimeric E6-E6AP-p53 complex, the p53 is targeted for destruction. In this way, reducing p53 activity promotes DNA replication in infected cells and enhances cell survival while suppressing apoptosis and promoting carcinogenesis. Furthermore, E6 has the ability to destroy other cellular proteins involved in the apoptotic signaling cascade, such as Bak, FADD, and procaspase 8[24,25].

As illustrated in Figure 9, the combined actions of E6 and E7 oncoproteins result in a synergistic impact that leads to an unregulated rise in cell proliferation, which leads to carcinogenesis.

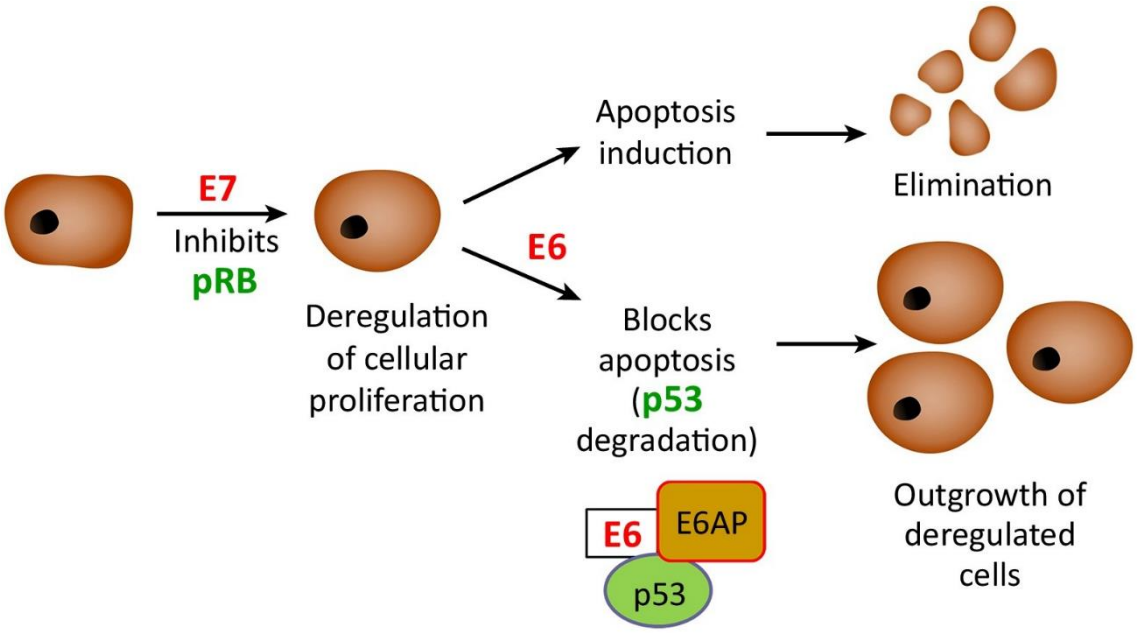

Figure 9 - Synergetic effect of the HPV E6 and E7 oncoproteins[22].

1.6. Current therapies

Cancer continues to be a highly lethal disease on a global scale. The existing treatments for cervical cancer include chemotherapy, radiation and surgery. However, these treatments have shown limited success rates, being effective in localized early-stage tumours and rarely prove to be effective in advanced stages or when metastasis had already occurred. Consequently, there is a pressing need for the development of novel therapeutic approaches that can provide durable protection and selectively target cancer cells, such as DNA vaccines, gene therapy and drugs with high anticancer capacity.

Nowadays, there are available three commercial prophylactic vaccines that offer protection against the main high-risk HPV types. Even though HPV vaccines have been widely available since 2006, vaccine acceptability has been low in many countries and, latterly, it has dropped in some countries where the vaccination rates were initially high. Besides, these vaccines are only prophylactic and are one of the most expensive to produce, being really difficult to distribute them in low-income countries, where most cases of HPV-associates diseases occur. In this sense, new therapies are needed and are being studied to find an effective, specific and affordable way to prevent or treat cervical cancer[24,26]. Such vaccines are summarized in Table 4.

Table 4- Current vaccines against HPV[26].

Vaccine	HPV type
Cervarix	16,18
Gardasil	6, 11, 16, 18
Gardasil 9	6, 11, 16, 18, 31, 33, 45, 52, 58

These investigations involve DNA- or RNA-based gene treatments, which have enormous promise but are prohibitively expensive, restricting their utility in the real world. Other therapies, such as the utilization of natural substances, have been investigated in this case due to their low cost and toxicity when compared to other chemical molecules[27]. Flavonoids are natural chemicals with significant anticancer activity, with prospective use in the treatment of cervical cancer due to their capacity to block the E6 oncoprotein, as in the instance of taxifolin[27].

1.7. Flavonoids

Flavonoids are a group of natural polyphenol compounds and can be found in vegetables, plants, fruits, grains and tea and are normally produced as secondary metabolites. Flavonoids are portrayed by having a skeleton base of C_6-C_3-C_6, which forms two aromatic rings (A and B) linked by a third heterocyclic pyran ring (©), as represented in Figure 10[28]. When flavonoids have an open C ring, they are called chalcones.

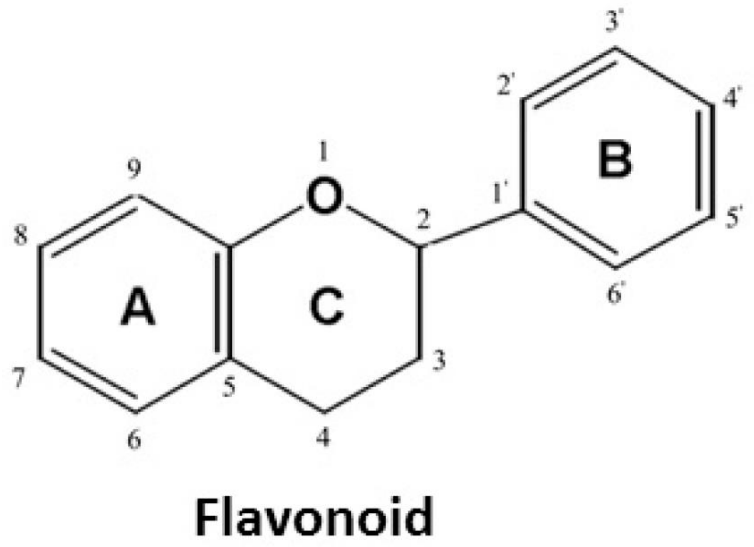

Figure 10 - Basic chemical structure of flavonoids[28].

These compounds have a widespread use as dietary complements and are considered scientific relevant, being stated as antidiabetic, anti-inflammatory, antimicrobial, antiviral and anticancer agents. However, the main biological activity of flavonoids is their antioxidant activity, which has been extensively explored and is well documented in literature[29].

Nowadays, the major focus revolves around the application of flavonoids in anticancer therapies. Some flavonoids such as quercetin, taxifolin, luteolin, apigenin, naringenin and silibinin have been reported as potential flavonoids in anticancer therapies. These flavonoids illustrated significant anticancer capacity, particularly

through some mechanisms like reduction of oxidative stress, increased antioxidant activity, induction of apoptosis and cytotoxic activity and carcinogen inactivation[29,30].

Even though the mechanisms that play a part in the anticarcinogenic potential of flavonoids have been reported, the several pathways leading to each one of them is not fully understood yet. So, research has been conducted to fully understand and unlock the processes of action of flavonoids to improve their effect and reduce their limitations.

As previously stated, one of the most essential roles of flavonoids is to reduce oxidative stress. When the balance of cellular homeostasis between pro-oxidant activity and antioxidant defense is disturbed, free radicals accumulate[31]. ROS are predominantly produced as byproducts of cellular oxidative phosphorylation in the mitochondrial electron transport chain. This increase in ROS levels causes oxidative stress, which is involved in the beginning and progression of inflammatory processes, as well as various degenerative illnesses and cancer[32].

Flavonoids have a dual action regarding ROS homeostasis, acting as antioxidants under typical physiological conditions and as a potent pro-oxidant in cancer cells, leading to a reduction in cell proliferation and, consequently, proto-oncogenes, thus decreasing the risk or retarding the progression to more perilous stages of cancer[29,33].

The ability to induce apoptosis is another crucial mechanism that flavonoids can do. There are two main signalling cascades of apoptosis, the extrinsic and the intrinsic pathway. The caspase 8 is the main signaling protein in the extrinsic pathway, which is connected to the tumour necrosis factor (TNF) superfamily. The intrinsic pathway, also known as the mitochondrial pathway, is linked to Bcl-2 family proteins, which subsequently activate caspase 9. Both caspases 8 and 9 will lead to an increase in caspases 3, 6 and 7, inducing apoptosis, as shown in Figure 11.

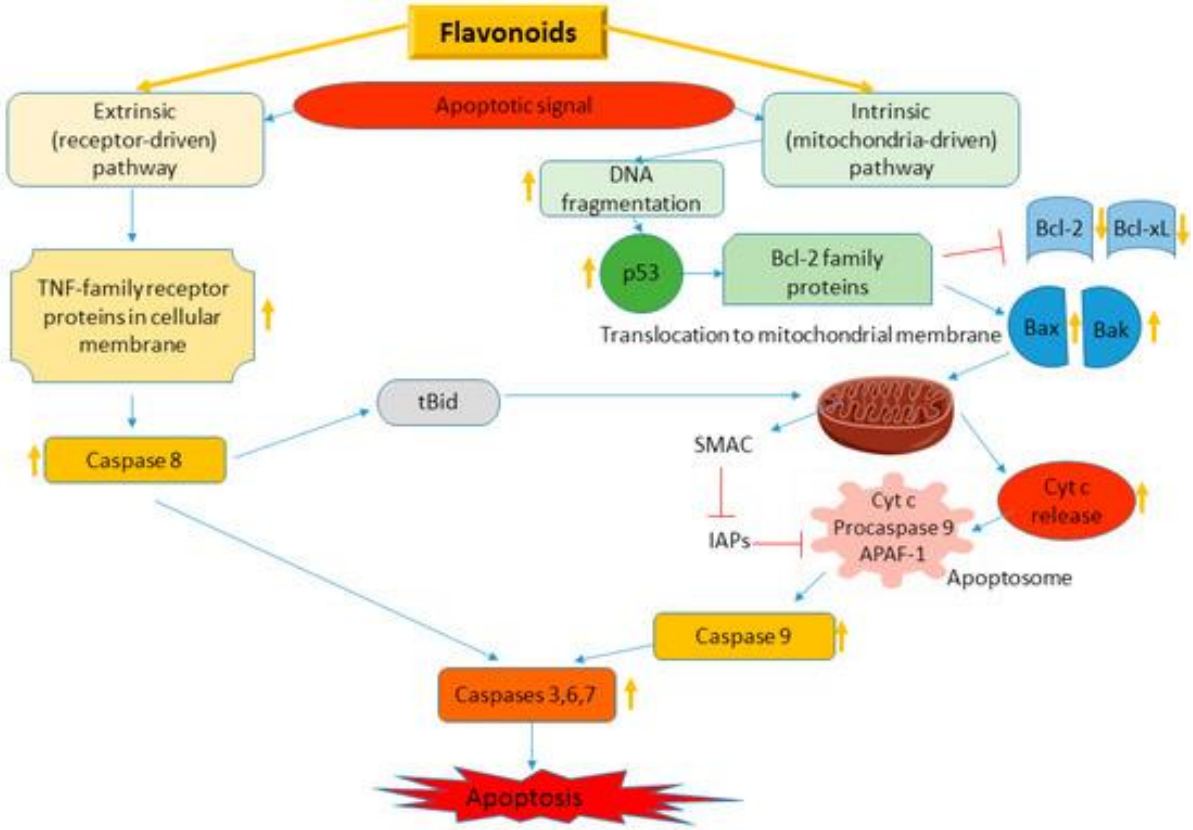

Figure 11 - Apoptotic pathways mediated by flavonoids[30].

Some flavonoids also have a major anti-cervical cancer mechanism, notably the suppression of the E6 oncoprotein. As previously stated, inhibiting this oncoprotein causes a rise in p53 levels, which leads to an increase in apoptosis induction via the intrinsic pathway. When compared to other types of cancer, this apparatus shows a specific and amplified action of flavonoids in cervical cancer, expanding its potential applications[34]. Taxifolin is a flavonoid that has shown potential to inhibit the E6 oncoprotein[27].

Furthermore, the use of flavonoids as chemotherapeutic adjuvants has been extensively researched. The use of this type of therapy enhances the intercellular accumulation of the medication in cancer cells, resulting in a significant reduction in the growth of these cells. Flavonoids have also helped to minimize toxicity in healthy cells. The combination of flavonoids and anticancer medications may overcome one of chemotherapy's most significant limitations, increasing the drug's anticancer activity even at low concentrations.

1.8. Flavonoids subgroups

As mentioned earlier, flavonoids are a class of polyphenols. They can be classified in accordance with their biosynthetic origin, as well as based on the aromatic ring binding site and the degree of saturation and oxidation of carbons that are present between the two rings. Based on their differences, flavonoids can be divided into 7 major groups[33], as illustrated in Figure 12, and their characteristics are described below.

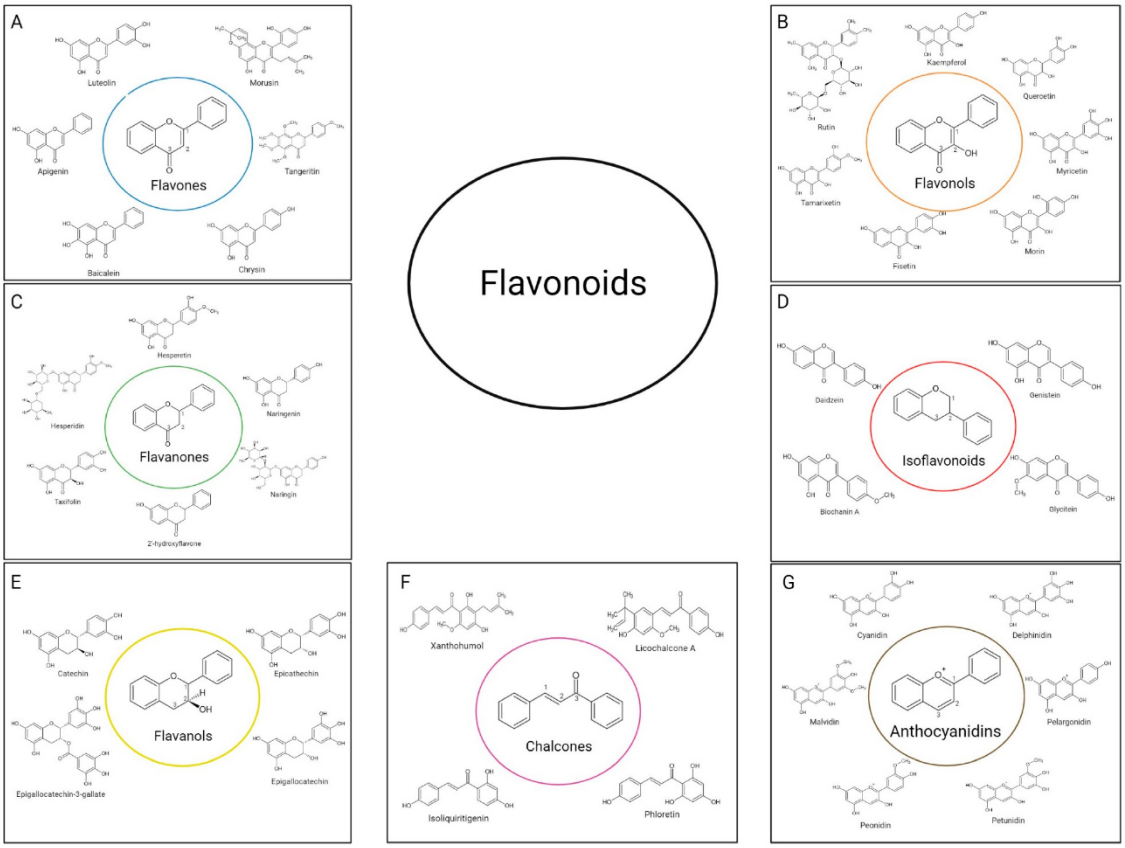

Figure 12 - Flavonoids classification: (**A**) flavones, (**B**) flavonols, (**C**) flavanones, (**D**) isoflavonoids, (**E**) flavanols, (**F**) chalcones, (**G**) anthocyanidins[33].

1.9. Flavones

In the form of glucosides, flavones, a large subclass of flavonoids, are widely distributed in leaves, flowers, and fruits. Some of the main sources of flavones include mint, chamomile, red peppers, parsley, celery, and peppers. Some of the most researched flavonoids, like luteolin and apigenin, are part of this subgroup. The peels of citrus fruits, particularly those with the polymethoxylated flavones tangeretin and sinensetin, are particularly abundant in these compounds. A double bond between positions 2 and 3 and a ketone group at position 4 of the C ring define flavones. For this reason, they are largely used in the food industry[28].

Regarding human beneficiary, flavones can decrease ROS production, inducing apoptosis and may interact with oestrogen receptors, preventing them to distort and thus binding to carcinogenic co-activators[35,36].

1.10. Flavonols

The subclass of flavonoids known as flavonols differs from flavones principally by having a higher degree of oxidation, which can be seen in Figure 12B by the presence of a hydroxyl group (-OH) on carbon 2.

Flavonols are abundant in nature and can be found in a variety of foods and drinks, including red wine, black and green tea, as well as fruits and vegetables like bananas, apples, onions, broccoli, and grapes. Additionally essential for plant growth, development, and physiological response in their native habitat, flavonols give plants resistance to insects and ultraviolet rays. Due to their antioxidant, antibacterial, anti-inflammatory, cardiovascular, and anticancer properties, flavonols are significant in terms of human health[36].

Among the various flavonols, quercetin stands out as a highly prominent subject of scientific investigation and therapeutic research. However, there are other flavonols with great potential, such as rutin, myricetin and fisetin[28]. Quercetin possesses the ability of increasing p53 levels by suppressing the E6 oncoprotein by binding to E6, thereby blocking the binding of E6 with E6AP, preventing its function[34,37].

1.11. Flavanones

The saturated and deoxidized carbons in flavanones—represented in Figure 12C by the numbers 1 and 2—are what give them their unique properties. They are the main byproducts of the flavonoid biosynthesis pathway and are renowned among the several flavonoid groups for being extremely reactive. Fruit skins, seeds, barks, and flowers are the main sources of this category of compounds[38,39].

Some of the important flavanones include taxifolin, hesperidin, and naringenin, which have antioxidant and anti-inflammatory properties[40].

Taxifolin has shown anti cervical cancer properties mediated by E6 oncoprotein activity[27,41]. Studies show that taxifolin was able to induce BAX protein activity in resemblance to the p53 protein results, suggesting apoptosis induction on HPV positive cell line, such as HeLa cells. In HPV-negative cell lines, taxifolin did not affect BAX protein levels, suggesting taxifolin inhibits the E6-dependent degradation of p53[27].

1.12. Flavanols (Flavan-3-ols)

The numerals 1, 2, and 3 in Figure 12E represent a structure that is present in flavanols, also known as flavan-3-ols, and in which the carbons are entirely saturated.

Among the members of this class, catechin, epicatechin, epigallocatechin, and epigallocatechin-3-gallate are the most well-known substances. This category is additionally known as catechins due to its structural characteristics. Although they can also be found in apples, chocolate, and cocoa, flavanols are mostly found in tea leaves[33].

Flavanols have been recognized for their capacity to reduce the activity of various digestive enzymes, including -amylase and -glucosidase, which has implications for human health. Additionally, flavanols have demonstrated an influence on blood pressure, lowering it efficiently and lowering the risk of cardiovascular disease[33,42].

1.13. Isoflavonoids

Isoflavonoids are secondary metabolites that are found in plants, particularly soybeans, red clover, and chickpeas. These substances play a crucial part in guarding the plants from pathogenic invaders. Due to the presence of a phenol group bonded to carbon number 2 rather than carbon number 1, as seen in Figure 12D, isoflavonoids structurally differ from other flavonoid families. They can exist in both glycosylated and aglycosylated aglycone forms. These substances have demonstrated promise in the prevention of diseases like diabetes, Alzheimer's disease, Kawasaki's syndrome, and heart disease, among others[43,44].

Additionally, isoflavones can bind to estrogen receptors because to their structural resemblance to estrogens, competing with cancer-related estrogens and lessening their effects[43,44].

1.14. Chalcones

Chalcones stand out as a distinct category of flavonoids in terms of chemical makeup due to the unusual arrangement of carbons denoted by numbers 1, 2, and 3 in Figure 12F. These carbons do not create a third ring between the two benzyl rings like other flavonoids do. Chalcones also contain a ketone group at carbon number three. The Moraceae, Leguminosae, and Compositae groups of plants frequently include this specific family of open-chain flavonoids. They can be found in a variety of plant products, including fruits, vegetables, cereals, flowers, roots, teas, and wines. Licochalcone A, phloretin, and isoliquiritigenin are notable chalcones[45].

Chalcones display a remarkable capacity to defend plants in their native habitat by efficiently scavenging ROS. This protective mechanism shields against attacks from bacteria and assists in preventing molecular damage. Chalcones have also been thoroughly researched for their therapeutic qualities, including, among others, their antifungal, anti-inflammatory, antibacterial, antiviral, anticancer, and neuroprotective activities[46].

1.15. Anthocyanidins

Anthocyanidins are the only group that is significantly soluble in water, and they have the distinctive property of having an unsaturated ring sandwiched between the two benzyl rings, which leads to the formation of a flavylium cation, as shown in Figure 12G. The pigments in leaves, flowers, vegetables, and fruits of plants contain a variety of these compounds. Additionally, anthocyanidins have exceptional qualities like the capacity to control physiological phases in plant tissues and inhibit ROS. This group of flavonoids contains some of the best-known flavonoids, such as cyanidin, malvidin, peonidin, and petunidin[47].

Anthocyanidins have been acknowledged for their numerous positive effects on human health. They have anticancer, anti-inflammatory, antidiabetic, anti-oxidant, and neuroprotective properties[47].

1.16. Flavonoids limitations

Although different flavonoids groups differ in this aspect, flavonoids generally have low toxicity and significant therapeutic value, but their bioavailability is quite low. With the exception of the anthocyanidins, which exhibit notable aqueous solubility, none of the other groups of flavonoids have much solubility in water. Due to the severe limitations on their oral absorption, both their bioavailability and therapeutic efficacy are decreased. Additionally, flavonoids are subject to extensive metabolism, low stability, intestinal permeability limitations, and degradation in highly acidic environments, all of which contribute to their overall low bioavailability[48].

Numerous delivery system-based approaches are actively being researched as ways to address these issues. These methods emphasize increasing intestinal absorption, enhancing stability, and changing the absorption site[49]. In addition to improving flavonoid solubility, delivery systems can also lessen gastrointestinal degradation, increase bloodstream absorption, stop renal clearance, and guard against hepatic excretion. As a result, research into how to accomplish this has drawn considerable scientific attention. Such delivery systems have the enormous potential to overcome these bioavailability constraints, releasing flavonoids' full therapeutic benefits and opening the door for their efficient use in a variety of applications.[50,51].

1.17. Delivery systems

As previously stated, a wide range of delivery systems is currently being developed for anticancer therapy. These innovative systems offer the opportunity to utilize lower concentrations of flavonoids while efficiently delivering them to cancer cells using specific ligands. This approach minimizes the risk of toxicity to healthy cells and maximizes the therapeutic benefits. Several delivery systems can be from different natures, being the main groups summarized in figure 13.

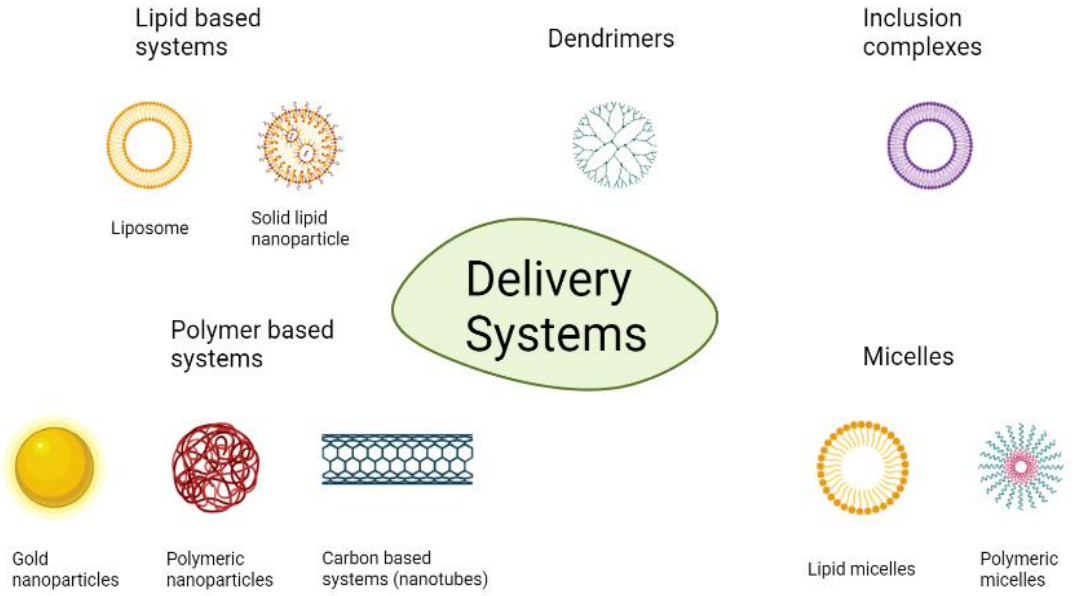

Figure 13 - Foremost types of delivery systems currently under development for the encapsulation of flavonoid[33].

1.18. Lipid based delivery systems

Liposomes, emulsions, and lipid-based nanoparticles are the three major types of lipid-based delivery methods, with minor divisions within these groups.

1.19. Liposomes

The main component of a liposome is a spherical vesicle that is typically created by emulsifiers and a bioactive substance that has been dissolved in an organic solvent. These delivery systems can be used to encapsulate both hydrophilic and hydrophobic drugs because they typically consist of at least one lipid layer. Phospholipids make up the majority of liposomes, but they can also contain cholesterol and/or hydrophilic materials like polyethylene glycol (PEG). Liposomes that have PEG incorporated into them are known as stealth liposomes because they circulate for a longer period of time, increasing their overall efficacy. When phospholipids and cholesterol are used to create liposomes, they typically offer structural and biological stability, resulting in biocompatible

transport systems with high flavonoids encapsulation efficiency. The encapsulation efficiency frequently exceeds 80%[52].

Because they tend to be stable, liposomes don't tend to aggregate, making them safe for therapeutic use. Additionally, the encapsulated flavonoids can be released in a controlled manner thanks to liposomes. However, because flavonoids naturally possess certain physical and chemical characteristics, there may be some issues with drug aggregation and degradation over time while being stored. Despite these difficulties, the advantages of liposomes include their size (typically between 100 and 200 nm) and polydispersity index (PdI), which ranges from 0.1 to 0.25. These characteristics allow liposomes to travel through blood capillary pores and collect in tumours, which typically have more capillary pores surrounding them[53].

Numerous therapeutic benefits of using liposomes have been consistently shown by both *in vitro* and *in vivo* studies, particularly their remarkable ability to encapsulate flavonoids. This ability to encapsulate results in a greater therapeutic effect while lowering potential toxicity. Studies on the viability of cervical cancer cell lines (HeLa) have shown that the concentration of flavonoids needed to reach a half inhibitory concentration (IC50) is reduced when they are encapsulated within liposomes[54].

The application of liposomes has also been explored for other types of cancer, demonstrating high encapsulation values, low toxicity, and substantial cell inhibition percentages in *in vitro* studies. Besides, various emulsifiers, mainly lecithin or PEG derivatives, have been extensively tested in anticancer therapies. In some cases, chitosan coatings have been investigated to improve bioavailability and stability *in vivo*, opening new possibilities to enhance the utilization of these type of systems in cervical cancer research[54].

1.20. Emulsions and nanoemulsions

Consideration should also be given to emulsions and nanoemulsions as delivery methods. Emulsifying agents like polyglyceryl-10 laurate or PEG 660-stereate are used in this particular class to take advantage of the interaction between water and oils. The objective is to develop systems that improve flavonoids' solubility and bioavailability. The thermodynamic instability of emulsions and nanoemulsions, which may experience some dissociation over time, should also be noted. However, they have some distinct advantages, such as a high flavonoid encapsulation efficiency that typically exceeds 80%, a decreased propensity for aggregation, and the prevention of gravitational separation[55]. Emulsions and nanoemulsions differ between themselves mainly by their size, with emulsions having a size greater than 200 nm, whereas nanoemulsions exhibit sizes below 200 nm. By adjusting the ratios of emulsifying agents, it is possible

to tailor the size range of these systems to achieve optimal targeting and accumulation at specific sites of interest[56,57].

1.21. Lipid based nanoparticles

Another category of nanoparticles that has undergone extensive research is lipid-based ones. These solid lipid structures are created at room temperature. Solid lipid nanoparticles (SLNs) and nanostructured lipid carriers (NLCs) are included in this subcategory. In contrast to NLCs, which have a non-ideal crystal structure that results in systems with both solid and liquid regions, SLNs have an entirely solid structure with a clearly defined crystal lattice. This distinguishes SLNs from NLCs. This distinguishing feature of NLCs enables a higher drug loading capacity and a lower water content58. SLNs, as opposed to liposomes, do not require organic solvents, which reduces cytotoxicity while maintaining a notable ability to encapsulate both hydrophilic and hydrophobic drugs. The excellent bioavailability, cost-effectiveness, scalability, and controlled release capabilities of SLNs are as a result of these factors[58].

Regarding composition, both SLNs and NLCs consist primarily of non-ionic surfactants, such as Poloxamer 188, Tyloxa-pol and sometimes lecithin or phosphatidylcholine, as these amphoteric components contribute to the system´s stability. NLCs can also incorporate liquid lipids, such as oleic acid, olive oil and almond oil, to form the liquid portion of the system. Despite the numerous advantages previously stated and their compatibility with *in vitro* and *in vivo* assays due to their natural composition, it is crucial to consider the potential toxicity of surfactants and other excipients required for their production. Additionally, the risk of aggregation and recrystallization remains within this type of delivery system[58,59].

1.22. Polymer based nanoparticles

Polymer-based delivery systems have been the most commonly researched and used for flavonoid encapsulation. Typically, such delivery systems are made up of nanoparticles and spherical walls with an outer polymer and a core made up of a hydrophobic surfactant that offers most flavonoids with good stability, solubility, and bioavailability[60,61]. This type of delivery system takes advantage of the dissolution of flavonoids in an organic compound, frequently ethanol, which is then removed by evaporation under vacuum, lyophilisation, or spray drying, to reduce the system's cytotoxicity. The features of these nanoparticles can vary substantially depending on the type of polymer used, and they are then classed based on their nature, being divided into natural, synthetic, or inorganic-based polymers[62].

1.23. Natural polymers

Biopolymers, also referred to as natural polymer-based systems, provide a wide range of applications depending on the particular ingredients used in their creation. Proteins and polysaccharides are frequently used in biopolymers. Due to their natural origin, these polymers have high biocompatibility, biodegradability, and low toxicity, which allows for their widespread use in both *in vitro* and *in vivo* experiments. However, it is uncommon to only use protein- and/or polysaccharide-based systems. Combinations with other kinds of biopolymers, synthetic polymers, or polymers derived from inorganic materials are frequently taken into consideration. Chitosan, one of the most widely used polysaccharides, is frequently combined with proteins, other polysaccharides, or various kinds of polymers. It has been discovered that this method improves biocompatibility, biodegradability, and stability[63,64]. Chitosan also has mucoadhesive qualities, making it easier to deliver systems to particular mucosal sites with precision. An approach that is frequently used to produce systems with enhanced performance for *in vitro* and *in vivo* assays is the conjugation of various biopolymers. These systems typically have sizes under 200 nm, high levels of stability, and controlled drug release, making it easier to deliver drugs to target cells. Natural polymeric systems that incorporate polysaccharides are frequently used in conjunction with other polymers or inclusion complexes and represent a significant method for improving the bioavailability of systems[63,64].

Regarding the use of polysaccharides in cervical cancer research, their utilization mostly relies on the conjugation of chitosan with another polymer, such as quinoline or gliadin[65].

Incorporating various polymer types through conjugation not only reduces the size of the system but also leads to a higher encapsulation rate[63,64].

1.24. Synthetic polymers

Polyethylene glycol (PEG) is the most commonly used polymer in synthetic polymers, which are another category of polymer-based nanoparticles. In order to increase the solubility of flavonoids and achieve a higher rate of encapsulation, PEG is frequently combined with other types of systems. Even though PEG-based systems have a low rate of degradation and limited biocompatibility, the encapsulation rate is typically high, exceeding 90%. However, using a combination of polymers can significantly reduce these negative effects, allowing for their use in both *in vitro* and *in vivo* assays[66].

Studies have been conducted to explore anticancer therapies against cervical cancer using both *in vitro* and *in vivo* approaches. These studies involve the use of PEG systems combined with poly lactide coglycolide, poly e-caprolactone conjugated with PEG 1000 succinate and pluronic systems modified with gelatin[67].

Cell viability assays have also revealed that synthetic polymer-based systems can achieve low IC_{50} values. This is attributed to the extended circulation time in the bloodstream that these systems offer. Even more, these systems also demonstrate a high capacity for conjugation with specific ligands such as folic acid, which actively facilitates the targeting of cancer cells. This targeting is only possible due to the higher presence of folic acid receptors in cancer cells compared to healthy cells[68]. Some *in vivo* studies exhibited a notable reduction in tumour weight compared to the administration of the drug in free form[69].

1.25. Inorganic polymers

A wide range of applications are available for inorganic polymer-based delivery systems, particularly in the areas of drug delivery, tissue repair, hyperthermia, and magnetic resonance imaging. The systems primarily make use of nanoparticles made of substances like gold, copper, and occasionally iron oxide, which are frequently used as nanoparticles or nanotubes. Although the systems may encounter difficulties like aggregation, oxidation, low stability, and restricted biocompatibility, these problems can be successfully overcome by coating the systems with polymers like PEG or chitosan[70,71]. The incorporation of such polymers not only helps overcome these disadvantages but also provides a platform for the attachment of flavonoids and ligands, thereby enhancing the viability and functionality of these systems. In addition, the inorganic systems are featured by a small size when compared to other types of delivery systems, around 50 nm or less, and good encapsulation rates, ranging from 70% to 80%[72].

1.26. Micelles

Micelles are formed by amphiphilic molecules, which can then be classified as polymeric micelles or lipidic micelles based on their polymeric or lipidic character[73]. The hydrophobic core makes it possible to encapsulate therapeutic agents with high hydrophobicity and low solubility, which makes them the perfect platform for flavonoid encapsulation. Additionally, improved stability and controlled release of flavonoids are ensured by this encapsulation. The hydrophilic region of these molecules, which makes

up the hydrophilic outer part of micelles, offers improved stability and protection, increasing the system's bioavailability[74,75].

Micelles offer several advantages, including their reduced size (normally below 100 nm), high thermodynamic stability, high drug loading capacity, increased cellular uptake and ease of large-scale production. However, the formulation of these systems requires careful consideration of component ratios and extensive studies are yet necessary to identify the ideal ratio[76,77].

1.27. Inclusion complexes

Inclusion complexes are delivery systems characterized by having a host molecule that can bind to another molecule through non-covalent interactions[70]. These complexes can interact hydrophobically with flavonoids, effectively trapping them inside their internal cavity. The solubility, stability, and bioavailability of flavonoids are all improved by this unusual structure. The complexes' cone shape, which has open ends, creates an outer surface that is hydrophilic and an inner surface that is hydrophobic, which helps with the encapsulation process. The encapsulation rates typically hover around 100%[78,79].

However, inclusion complexes have their limitations. They may not be ideal for encapsulating larger flavonoids, especially those with glycosylation. Additionally, these complexes tend to be relatively large in size, often exceeding 200 nm, which limits their use in controlled delivery studies conducted both *in vitro* and *in vivo*. Consequently, their versatility is somewhat restricted and alternative and more cost-effective methods for flavonoids encapsulation are available[80].

Cyclodextrins make up the majority of this group of delivery mechanisms, with β-cyclodextrins being the most popular. These cyclodextrins can also have their physical and chemical properties changed to better suit particular delivery sites. β-cyclodextrins can be positively or negatively charged and have varying levels of substitution by going through chemical modifications. There are various kinds of -cyclodextrins, including β-cyclodextrin, carboxymethyl-β-cyclodextrin, sulfobutyl ether-β-cyclodextrin, and hydroxypropyl-β-cyclodextrin, with the latter being the type that is most frequently used in scientific studies. Additionally, cyclodextrins can be blended with other polymers, such as chitosan, to increase their stability, shrink their size, and boost their bioavailability.[81]. Moreover, the conjugation of cyclodextrins with biotin is common, as biotin receptors are often highly expressed in cancer cells, enabling a more effective targeting of cancer cells. In addition to β-cyclodextrins, other delivery systems based on inclusion complexes are being investigated for flavonoid encapsulation, such as α-cyclodextrins, γ-cyclodextrins and β-lactoglobulins[79,80].

1.28. Other types of delivery systems

Dendrimers are one of the most promising carriers among the alternative delivery systems that may be used to encapsulate and target flavonoids to cancer cells. Dendrimers are polymeric substances with an intricately branched structure, numerous functional groups, and an interior cavity that can encapsulate medications like flavonoids. Particularly, poly(amidoamine) dendrimers have received extensive study and application in numerous *in vitro* assays focusing on various types of cancer[74,82].

However, the application of dendrimers is still limited due to their inherent toxicity. To address this concern, approaches like PEG conjugation have been explored to minimize toxicity and establish a stronger association with specific ligands. Further investigations are needed to explore new strategies that can enhance the stability and bioavailability of dendrimer-based delivery systems, thereby improving their effectiveness in encapsulating flavonoids and facilitating their targeted delivery to the desired cells[83,84].

The emergence of nanotechnology in the biomedical area has opened up exciting prospects, particularly in drug vectorization research. Nanocarriers offer the potential to safeguard drugs against premature degradation, enhance their bioavailability, extend their presence at specific anatomical locations, thereby diminishing necessary dosages and extending dosing intervals. Chitosan, being the exclusive positively charged natural polysaccharide, has been widely used in drug delivery applications[85].

1.29. Chitosan

Over the span of a few years, nanomaterials have undergone a notable transformation. Which was initially regarded with just curiosity, has now become the focus of intense research and development, progressing swiftly, and reaching the point of commercialization and industrial relevance[86].

Biomass-based nanomaterials have garnered significant global attention as a thriving area of research due to their unique combination of intricate nanostructure design, biocompatibility, and sustainable sourcing, leading to extensive exploration and value derivation. Among the biomass-based materials, cellulose emerged as a pioneer, dominating both the number of publications and the wide range of applications that have been extensively studied and successfully commercialized[86].

However, more recently, researchers have opened their horizons and interest beyond cellulose and begun exploring alternative biomass sources capable of producing similar nanostructures. One natural alternative is chitin, which is the second most

abundant biopolymer worldwide, surpassed only by cellulose. Chemically, chitin is a linear polysaccharide consisting of repeat units of β-(1→4)-2-acetamido-2-deoxy-β-d-glucose, with a distinctive acetamide attached to the C2 position. Chitin is found in the shells of crustaceans, insects, and certain fungi, boosting an annual global availability in the order of billions of tonnes[86].

In contrast to chitin, chitosan, which is derived from chitin, has a slightly different chemical composition, consisting of repeating units of β-(1→4)-2-amino-2-deoxy-β-d-glucose and is characterized by having primary amine functionalities. The conversion of chitin to chitosan involves deacetylation. Typically carried out in basic conditions, where the acetamide groups in chitin are hydrolysed to form chitosan and acetic acid. To quantify the extent of deacetylation, a degree of deacetylation (DDA) measurement is commonly used. This chemical modification through deacetylation gives chitosan an advantage in terms of solubility in acidic and aqueous media compared to chitin. This enhanced solubility makes chitosan highly suitable for a variety of applications. Figure 14 shows the chemical structures of chitin and chitosan[86,87].

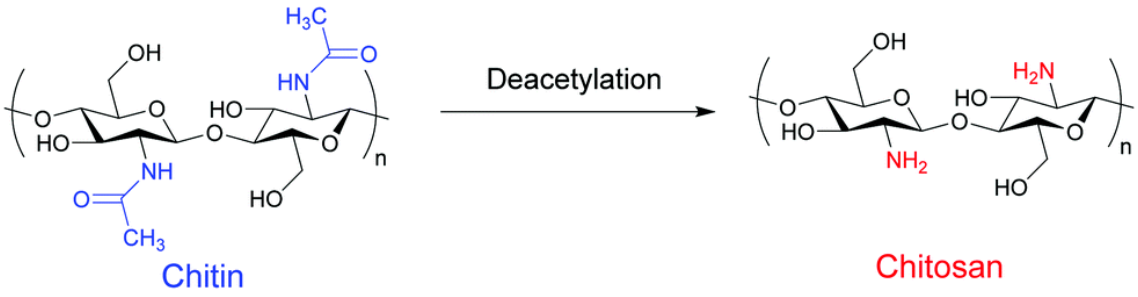

Figure 14 - Chemical structure of chitosan[86].

Chitosan, as previously mentioned, has high compatibility and biodegradability, low toxicity, a high mucoadhesive ability and a cationic nature. It also has antioxidant and antimicrobial properties. This versatility arises from its active amino groups, which serve as reactive sites for attaching a wide range of functional groups using mild reaction conditions. Additionally, the cationic nature of chitosan, stemming from its amino groups, makes it known as an amino polysaccharide. At low pH, chitosan remains as a polycationic polymer, due to protonation of amino group with increased solubility properties[88].

The cationic nature of chitosan allows its conjugation with anionic compounds, enabling the connection of the positive charges of chitosan with the negative charges of another compound by electrostatic interactions, such as TPP or gellan gum[89].

As already mentioned, chitosan polymers can vary its deacetylation degree, as well its molecular weight and the formulation method. These parameters will be

modified according to the type and site of the delivery system and also according to the drug to be encapsulated[88].

Regarding the DDA, is normally comprised between 30 and 95% and allows the presence of more or less amine groups, thereby potentially altering the ratios between amine and phosphate groups that are present in the system due to the other polysaccharide or crosslinker, leading to a change in the system's charge and facilitating cellular internalization[86].

Likewise, the use of a chitosan with a high molecular weight (HMW), normally higher than 200 kDa, promotes the creation of systems with larger sizes, thus allowing the encapsulation of bigger drugs. Alternatively, when considering low molecular weight (LMW) chitosan, usually smaller than 150 kDa, the systems tend to have smaller sizes, enabling the encapsulation of smaller molecules, being widely used for the encapsulation of DNA vectors[90].

Finally, the use of different formulation methods gives the possibility of varying the ratios between amine and phosphate groups on the surface of the delivery systems, along with a change in their size and shape. Furthermore, the use of chitosan conjugated with other compounds offers a wide range of delivery systems, allowing the encapsulation of several kinds of drugs, like flavonoids[91].

1.30. Chitosan-based formulation methods

Therefore, since there is the possibility of creating systems with unique characteristics, the most employed techniques include ionic crosslinking, polyelectrolyte complexation, precipitation or flocculation, solvent evaporation, spray drying and chitosan coating solution. These methods will be further elaborated upon in the following subsections, outlining their specific features and applications.

1.31. Ionic cross-linking

Ionic crosslinking is widely used for the formation of nanoparticles, particularly for chitosan-based ones. This technique involves adding a negatively charged compound to the chitosan solution. As a result, the positive charge of chitosan interacts with the negative charge of the crosslinker, facilitating the formation of delivery systems[92].

Ionotropic gelation is a specific form of ionic crosslinking where the negative charge compound is gradually introduced to the chitosan solution while the last one is being under agitation. This method is known for its simplicity and low cost. However, it has some drawbacks such as low stability of the resulting systems and a variable size distribution, needing the optimization of ratios between the chitosan and the crosslinker[92].

1.32. Precipitation or flocculation

This technique involves the preparation of nanoparticles by incorporating sodium sulfate as a precipitation agent. However, it is important to note that the precipitation method tends to result in the formation of delivery systems with a wide size range, which can limit their suitability for biomedical applications[92].

1.33. Solvent evaporation

The solvent evaporation technique relies on the varying volatility of solutes to create nanosystems. In this method, a surfactant is added to an organic phase containing chitosan, resulting in the formation of an emulsion. This emulsion is then stirred, allowing for the evaporation of the organic phase and the subsequent formation of nanosystems. Generally, these nanosystems exhibit a spherical and uniform morphology. The solvent evaporation technique finds extensive use in formulating nanosystems that encapsulate hydrophobic drugs[92].

1.34. Spray drying

In the formulation process of spray drying, chitosan and the desired drug are dissolved together, and, optionally, a crosslinker may be added to enhance stability. The resulting solution is then sprayed into a drying chamber, where the solvent evaporates, leading to the shaping of nanoparticles. These nanoparticles typically exhibit a uniform and spherical morphology, along with a relatively consistent size range. However, it is important to note that the use of hot air during spray drying can cause degradation of the encapsulated drug. This occurrence is particularly significant for compounds such as flavonoids, which are known for their poor stability[92].

1.35. Chitosan coating solution

This technique consists of incorporating a chitosan solution into an existing chitosan nanoparticle solution. Through this process, the nanoparticles become enveloped with an outer chitosan layer, resulting in a more uniform and spherical morphology. Additionally, this outer layer enables a controlled release of the encapsulated drug, enhancing the desired drug delivery of the nanoparticles. However, with the addition of chitosan, the nanoparticles size tends to increase[92].

1.36. Polyelectrolyte complexation

Coulomb's (electrostatic) interactions between charged microdomains of two oppositely charged polyionic components give rise to the formation of polyelectrolyte

complexes (PECs). These complexes exhibit optical homogeneity and stability, resulting in nanodispersions with colloidal dimensions. One of the most important advantages of PEC formation is the avoidance of a chemical cross-linking agent, which helps mitigate potential toxicity and unwanted effects normally associated with such reagents[93].

PECs can possess diverse structures and properties, making them highly versatile for a wide range of applications in various fields. They find utility in medicine, pharmacy, biotechnology, tissue engineering, biomaterials, biomedicals, cosmetics, and more. This is largely due to their biodegradable, biocompatible and non-toxic nature, making them of significant interest in pharmaceutical and biomedical research[94].

PECs are typically prepared at room temperature by utilizing a polycation or polyanion as the initial solution. The process of forming the complex can generally be achieved in two ways. The first approach involves the gradual addition of the polyanionic solution, drop by drop, at a predetermined flow rate to a polycationic solution. The second approach entails a rapid, one shot addition of one polyelectrolyte solution to an oppositely charged polyelectrolyte of similar ionic strength, while maintaining a constant speed magnetic stirring. Both approaches enable the controlled and efficient formation of PECs under carefully controlled conditions, facilitating their subsequent use in various applications[95].

The physicochemical characteristics of the complexes formed when chitosan interacts with other polyanions are significantly influenced by several factors that include the inherent properties of the parent polyelectrolytes, such as the type of charges present and the charge density along the polymer chains. Additionally, the conformation of the polymer chains in solution plays a crucial role in shaping the behaviour of these complexes. This conformation is influenced by the intrinsic characteristics of both polymers[85].

Gellan gum (GG) has been researched for the preparation of polyelectrolyte complex nanoparticles in different ratios of GG to chitosan[96]. As GG carries negative charges when dissolved in water, chitosan is a promising choice for use as a positively charged groups to create electrostatic interactions between oppositely charged chains and thus produce nanoparticles[97].

1.37. Gellan gum

The ability of certain microorganisms to produce biopolymers through fermentation provides a valuable source of materials with remarkable technological properties. These microbial exopolysaccharides are increasingly getting recognized as valuable components in a range of human-made products across industries such as chemicals, pharmaceuticals, cosmetics, and food manufacturing. Notably, these

biopolymers offer the advantages of easy availability, environmental friendliness and are bioresorbable[98].

Among the various microbial exopolysaccharides, gellan gum (GG) stands out as a widely used biomaterial due to its affordability and consistent quality, which allows for large-scale industrial production. GG is a water-soluble polysaccharide produced by the bacterium *Sphingomonas elodea*. While is traditionally employed as a stabilizer, thickener, viscosifier and gelling agent, the unique nature of GG opens up exciting possibilities for exploring alternative applications. Gellan gum is approved by FDA and is widely used as a food additive and beverage fortification due to its non-toxicity[99].

This diverse range of potential applications for GG stems from its properties. GG can form gels in the presence of divalent cations, such as calcium, making it a promising candidate for use in tissue engineering, drug delivery systems and encapsulation of bioactive compounds[100]. Gellan gum is a linear anionic polysaccharide and is comprised by a backbone of repeating unit of [β – 1,3 – D – glucose, β – 1,4 – D – glucuronic acid, β – 1,3 – D – glucose, α – 1,4 – L – rhamanose] and two acyl groups, acetate and glycerate bound to the glucose residue adjacent to glucuronic acid. The percentage of the main constituents is approximately 60% glucose, 20% rhamnose and 20% glucuronic acid. Figure 15 shows the chemical structure of gellan gum[99].

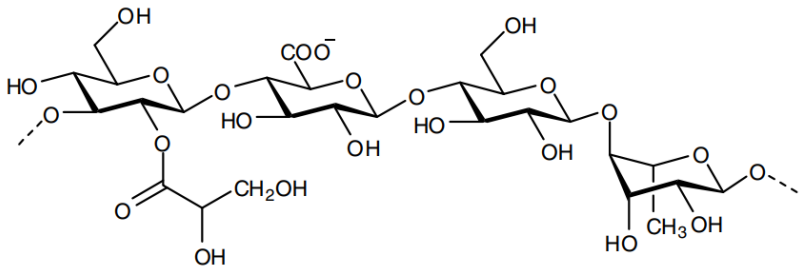

Figure 15 - Chemical structure of gellan gum[99].

Studies have been developed based on GG and CH through the formation of PECs, allowing nanoparticles to be formed with the ability to encapsulate drugs, like taxifolin[101,102].

1.38. Taxifolin

Taxifolin, also known as dihydroquercetin or 3,5,7,3,4-pentahydroxy flavanone, is a flavonoid commonly found in onions, milk thistle, Douglas fir bark and French maritime pine bark, as well in many plants[103].

The basic structure of taxifolin consists of two phenyl groups (rings A and B), which are joined together by a heterocyclic ring (C) and its chemical structure is shown in Figure 16[104].

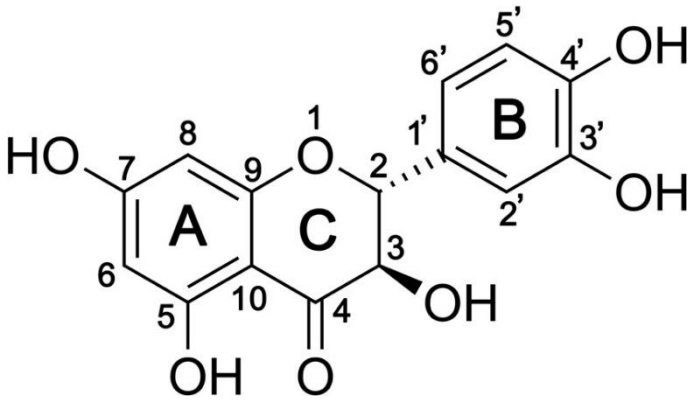

Figure 16 - Chemical structure of taxifolin[104].

Taxifolin differs from quercetin in one single structural element, which is the presence/absence of a C2, C3-double bond in the C ring. Taxifolin is considered an antioxidant and meets two of the criteria for effective radical scavenging ability, which are the presence of the o-dihydroxy structure in the B ring conferring stability and the 5- and 7-OH groups with 4-oxo function in the A and C rings that are responsible for a maximum radical scavenging potential. However, it lacks the 2,3 double bond in the C ring rendering it less potent than other flavonoids, like quercetin[105].

Taxifolin is known for its anti-inflammatory[106], antimicrobial[107], hepatoprotective[108], cardiovascular[109], and anticancer activities. Within the anticancer activity, both *in vitro* and *in vivo* experiments showed promising results against breast[110], lung[111], colorectal[112] cancer.

HPLC analysis has revealed that taxifolin can exist in both *cis* and *trans* forms and that it crystallises as two independent molecules in a cell[113].

However, taxifolin has a very limited bioavailability due to its slight water solubility (0.1% at room temperature), making it very difficult for taxifolin to be absorbed and metabolized, compromising its efficacy[104,105].

2. Objectives

The aim of this master's dissertation is to develop suitable delivery systems for taxifolin encapsulation, one of the main flavonoids with a proven carcinogenic and E6 oncoprotein inhibition effect, improving its bioavailability. Therefore, some techniques have been explored to enable taxifolin encapsulation and promote its delivery to target cells.

Different delivery systems were explored, considering three different types of chitosan, all combined with gellan gum. Several ratios, between these compounds, were considered at formulation step and then evaluated in order to select the one that gives rise to the most favourable properties, namely a reduced size and PdI, a positive surface charge, a uniform and spherical morphology, a high encapsulation efficiency and good releasing profile.

The system that presents the most suitable properties will be tested in cell assays, namely cell internalization to monitor its ability to enter the cells and promote taxifolin delivery.

3. Materials and methods

3.1. Materials

High molecular weight chitosan (HMW CH), with a MW range between 200 and 500 kDa, was acquired from Heppe Medical (Halle, Germany). 5 kDa chitosan, low molecular weight chitosan (LMW CH), with a MW range between 50 and 190 kDa, gellan gum (Gelzan™, Gelrite®) and taxifolin were purchased from Sigma Aldrich Chemicals (St. Louis, MO, USA).

All solutions were freshly prepared using ultra-pure grade water, purified with a Milli-Q system from Millipore (Billerica, MA, USA).

3.2. Methods - Preparation of solutions

Stock solution of chitosan (LMW, HMW and 5 kDa, 1 mg/mL) was prepared by dissolving the chitosan in sodium acetate buffer (0.1 M, pH 3). The solution was then diluted in Milli Q water to a concentration of 0.1 mg/mL and 0.3 mg/mL.

Gellan gum (0.1 mg/mL) was suspended in Milli Q water at 80 °C for 30 min. Both chitosan and gellan gum solutions were filtered with a 450 nm filter and stored at room temperature until use.

Stock solution of taxifolin (1 mg/mL) was dissolved in 70% ethanol for 1 h in a dark chamber at room temperature. Taxifolin was then diluted until reach a concentration of 0.2 mg/mL.

Taxifolin was also dissolved in Milli Q water (0.2 and 0.4 mg/mL) in a dark chamber at room temperature for 30 min. All the taxifolin solutions were stored at 4 °C and were protected from light until use.

3.3. Preparation of chitosan and gellan gum systems

Chitosan and gellan gum systems (CH/GG) were formulated using the polyelectrolyte complexation technique. Briefly, the gellan gum solution was added to the chitosan solution (2mL), drop by drop, using the Apparatus system under continuous agitation at 500 rpm. Different concentrations of chitosan (0.1 and 0.3 mg/mL), different volumes of gellan gum (0.5, 1, 1.5 and 2 mL) and different flow rates (0.3 and 0.5 mL/min) were tested to assess the best formulation possible for the posterior incorporation of taxifolin.

CH/GG systems were then left for 30 min under agitation at room temperature to allow stabilization of the nanoparticles. The nanosuspensions obtained were used for the particle size and zeta potential analysis.

3.4. Preparation of taxifolin delivery systems

Taxifolin delivery systems (CH/GG/TAX) were formulated using the same technique described above. 2 mL of chitosan solution was put on stirring at 500 rpm. Then, 3 different volumes of taxifolin (0.1, 0.2 and 0.4 mL) at 2 different concentrations (0.2 and 0.4 mg/mL) were added to the chitosan solution, dropwise. Thereafter, gellan gum was added to the previous mixture, drop by drop, followed by continuous stirring for 30 min.

3.5. Nanoparticle size and zeta potential analysis

Nanoparticles characterization was performed by Dynamic Light Scattering (DLS) at 25 °C using the Zetasizer Nano ZS equipment (Malvern Instruments, UK) and the Malvern Zetasizer software. Each formulation was evaluated by measuring its size, PdI and zeta potential. 1 mL of sample was placed in a disposable cell, which was used to measure size and PdI. Zeta potential specific DTS 1070 cuvettes were used to measure the zeta potential. All samples were analysed in suspension immediately after preparation in order to avoid changes in size and charge due to Ostwald ripening or particle growth and all parameters evaluated were measured in triplicates from three independent samples and validated by the Zetasizer Nano ZS (n=3).

3.6. UV/vis Absorbance Spectrum

After formulation as previously described, the CH/GG systems were centrifuged at 14000 rpm for 10 min and the pellets were resuspended in water. UV/vis spectrum was acquired using a UV-vis spectrophotometer (Thermo Scientific™ Evolution 220, Waltham, MA, USA) with a range between 250 and 500 cm^{-1} in order to understand if CH/GG systems would interact between them and if there is a significant peak at 289 nm, which is the taxifolin peak[114].

3.7. Scanning electron microscopy

The morphology of the most favourable NPs was evaluated using a scanning electron microscopy (SEM). Delivery systems made with each type of chitosan were centrifuged at 9500 rpm for 12 min at 4 °C and the pellett was then resuspended in 200 µL of Milli-Q water and centrifuged again in the same conditions. This last step was made three times two ensure that all the impurities were removed. After the last centrifugation, the supernatant was removed and the nanoparticles were resuspended in 40 µL of tungsten 2%. Then, each sample was diluted 1:20 in ultra-pure water and 10 µL was placed in a circular coverslip. The samples were left drying overnight, at room

temperature. The next day, the samples were coated with gold using an Emitech K550 sputter coater. A SEM Hitachi S-2700 was used with an acceleration of 20 kV at various magnifications to evaluate the morphology of the delivery systems.

3.8. Fourier-transform infrared spectroscopy

Fourier-transform infrared spectroscopy (FTIR) study was performed for pure drug, pure polymers, CH/GG systems and CH/GG/TAX systems to evaluate the interaction between the compounds of the delivery systems. Regarding samples preparation, each formulation was centrifuged at 14000 rpm for 10 min at room temperature and the pellett was then resuspended in 400 µL of ultra-pure water. Each formulation was freeze dried and kept overnight at -80 °C and then lyophilized for 24 h using a ScanVac Coolsafe freeze dryer (Labogene, DK). The spectra were acquired using a Nicolet iD10 FTIR spectrophotometer (Thermo Scientific, Waltham, USA) with an average of 120 scans, a spectral width within the range of 4000-400 cm^{-1} and a spectral resolution of 32 cm^{-1}.

3.9. Encapsulation efficiency

To determine the encapsulation efficiency of the most favourable nanosuspensions obtained, the formulations were centrifuged for 10 mins at 14000 rpm and the supernatant was transferred to a Vivaspin concentrator with a MWCO of 10000 and centrifuged for 20 min at 5000 rpm at room temperature. The filtrate, which contained free taxifolin, was then analysed by HPLC.

For the taxifolin quantification by HPLC, 100 µL of each sample was injected in a C18 column (250 mm × 4.6 mm) and detected using a DAD detector at an ultraviolet wavelength at 289 nm. The mobile phase consisted of acetonitrile (50%) and 0.1% acetic acid in water (50%) and the column temperature was set at 25 °C. Taxifolin was identified by comparing the retention time of a standard sample and quantified it through calculating the area under the curve with the external standard. A calibration curve was previously obtained with standards concentrations of taxifolin dissolved in Milli-Q water (10, 25, 50, 75, 100, 150, 175 and 200 µM)[115]. The calibration curve is represented in figure 17.

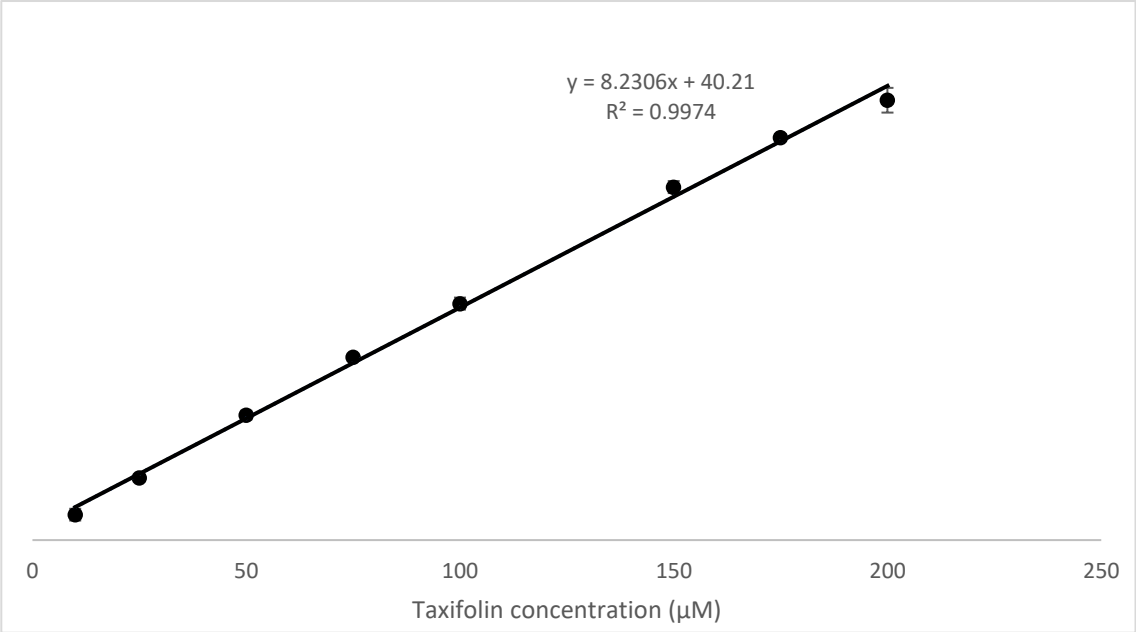

Figure 17 - HPLC calibration curve for taxifolin in water.

The encapsulation efficiency was determined by using equation 1. All the conditions were performed in three independent assays (n=3).

$$EE(\%) = 100 - \frac{Concentration\ of\ free\ taxifolin}{Concentraion\ of\ total\ drug} \times 100 \quad (1)$$

3.10. *In vitro* release studies

In vitro release studies were performed in a phosphate buffer saline (PBS). Delivery systems of each type of chitosan were centrifuged for 10 min at 14000 rpm. Then, the supernatant was transferred to a Vivaspin concentrator filter with a MWCO of 10000 and centrifuged for 20 min at 5000 rpm to wash and get loose of any free drug and recover system in suspension. The following retentate was then used to resuspend the previous pellett and was added PBS until the final volume of 1 mL. The sample was placed in an orbital agitator at 30 rpm and 37 °C, secured from light. At defined time intervals of 0, 2, 6, 12, 24, 48 and 72 h the sample was centrifuged using the same conditions as described above. This time, the filtrate was transferred to a 96-well plate (100 µL per well) and quantified through the absorbance at 289 nm, using the microplate reader Bio-Rad x Mark spectrophotometer (Bio-rad, EUA). The filtrate would resuspend the pellett and PBS was again added until 1 mL of final volume. A standard curve was previously obtained with standards concentrations (10, 25, 50, 75, 100, 125, 150, 175 and 200 µM) of taxifolin in PBS at the required pH. The releasing was calculated in a

cumulative way, i.e., the releasing at 6 h was obtained adding the release value at that defined time interval and the previous releasing values and so on. These assays were performed at two different pH values (7.4 and 5.8) to understand the release in normal physiological conditions and in acidic conditions that represents a tumor environment.

3.11. Cell culture

HeLa cells (HPV18 positive cervical cancer cells) and hFiB (fibroblasts) cells were cultured in Dulbecco's Modified Eagle's Medium/Ham's F-12 nutrient mixture (DMEM-F12), supplemented with 10% (v/v) fetal bovine serum and a mixture of penicillin (100 mg/mL) and streptomycin (100 mg/mL). Cells were grown in 25 cm^3 T-flasks at 37 °C and in a 5% CO_2 humidified atmosphere until 80% confluence was obtained.

3.12. Cell internalization

FITC-labelled chitosan was produced as described by Yuqing Ge and coworkers with slight modifications[116]. Briefly, 0.5 µL of FITC 100 mg/mL dissolved in DMSO was added to 10 mL of LMW chitosan (0.1 mg/mL in sodium acetate buffer 0.1M pH 4.5). The reaction was kept for 4h in dark conditions under agitation. After that, chitosan solution was washed with distilled water and centrifuged for 30 min at 12.000 rpm at 4 °C until no fluorescence was detected in the supernatant.

Then, the delivery systems assemblance was performed as described previously. After, the nanoparticles were centrifuged for 10 min at 14000 rpm. The formed supernatant was transferred to a Vivaspin concentrator with a MWCO of 10000 and centrifuged for 20 min at 5000 rpm to wash and get loose of any free drug and recover systems in suspension. The following retentate was used to resuspend the previous pellett and the nanoparticles were kept at -20 °C overnight. At the next day, delivery systems were resuspended with PBS and applied at 120 µM.

HeLa and hFiB cells were seeded in an 8-well µ-slide (Ibidi, Martinsried, Munich, Germany) at a concentration of 15625 and 31250 cells/well for 24 h, respectively. Therefore, media was discarded and replaced by free media (0% FBS) for an overnight incubation. At the next day, FITC labelled LMW CH/GG/TAX systems were resuspended in free media and applied to the cells. At defined intervals of 0, 2, 4 and 6 h of transfection, cells were visualized using LSM 710 Confocal Laser Scanning Microscope (Carl Zeiss, Oberkochen, Germany) under 63× magnification. To better understand cells' locations, nuclei were stained with DAPI 1:1000. DAPI was applied 10 min before the first visualization.

4. Results and discussion

4.1. Development of chitosan and gellan gum systems

Polymeric nanoparticles have been a material of choice for delivery of active compounds due to their biodegradability, biocompatibility, good encapsulation efficiencies and stability.

According to the literature, one of the factors that most influences the cellular internalization is the size of the delivery systems. It is desirable that delivery systems ideally have a size smaller than 200 nm, although they can reach up to 500 nm depending on the type of system under study and its application[117].

PdI is also an important property that quantifies the degree of size distribution or heterogeneity of particles in a sample. It is a dimensionless value ranging from 0 to 1. A PdI of 0 indicates a fully monodisperse system where all the particles have the same size, while a PdI of 1 refers to a very polydisperse system with a wide range of particle sizes. A lower PdI value suggests a narrower size distribution and greater uniformity among the nanoparticles, with regarding to the size. Generally, a PdI value below 0.3 indicates relatively homogeneous or monodisperse nanoparticles[118].

Another important factor that influences cellular internalization is the surface charge of the delivery systems. Positively charged nanoparticles are the most efficient at cell membrane entry and cellular internalization due to their effective binding to the negatively charged groups on the cell surface. Normally, values around +30 mV are recommended because it favours electrostatic interaction and avoid toxicity and agglomeration[119].

However, it is also known that polymer concentration influences the particle size and the zeta potential of nanoparticles. Thus, in the beginning, low molecular weight chitosan and gellan gum (CH/GG) systems were formulated to see if the polymers would interact between them and form adequate nanoparticles. Both polymer's solutions were adjusted to pH 4.5 before being mixed due to the biggest difference between their charges, favouring electrostatic interactions[102].

As previously mentioned, to determine the most favourable formulation for the subsequent incorporation of taxifolin, several variables were tested such as chitosan concentration, gellan gum volume and flow rate, (*i.e*, the dropping speed of the gellan gum solution when is adding to the chitosan solution). Chitosan volume (2 mL) and gellan gum concentration (0.1 mg/mL) remained constant through the whole procedure.

Characterization studies based on the determination of size, PdI and zeta potential of the resultant nanoparticles were carried out by the Zetasizer Nano ZS

equipment to assess the best ratio of CH/GG. All the results were made in triplicate (n=3) and are presented in table 5 and figure 18 for better visualization.

Table 5- Preparation conditions, mean size, PdI and zeta potential of CH/GG systems.

Chitosan concentration (mg/mL)	Gellan gum Volume (mL)	Flow rate (mL/min)	Size (nm)	PdI	Zeta Potential (mV)
0.1	**0.5**	**0.5**	**238.07 ± 31.18**	**0.29 ± 0.08**	**+22.56 ± 2.83**
0.1	1	0.5	267.89 ± 19.39	0.29 ± 0.12	+27.01 ± 4.12
0.1	1.5	0.5	269.59 ± 08.45	0.25 ± 0.07	+28.74 ± 5.17
0.1	2	0.5	317.48 ± 53.27*	0.24 ± 0.08	+29.75 ± 4.14
0.3	**0.5**	**0.5**	**221.98 ± 22.33**	**0.51 ± 0.04***	**+21.36 ± 7.67**
0.3	1	0.5	270.57 ± 16.81	0.47 ± 0.02	+21.93 ± 7.99
0.3	1.5	0.5	307.05 ± 77.39*	0.41 ± 0.06	+28.65 ± 11.17
0.3	2	0.5	307.25 ± 24.45*	0.36 ± 0.07	+26.07 ± 7.97
0.1	0.5	0.3	308.40 ± 78.57*	0.35 ± 0.09	+18.97 ± 5.37
0.1	1.0	0.3	278.41 ± 38.37	0.36 ± 0.09	+27.57 ± 4.75
0.1	1.5	0.3	288.82 ± 26.09	0.23 ± 0.10	+30.35 ± 5.10
0.1	2.0	0.3	317.78 ± 10.57*	0.27 ± 0.12	+30.07 ± 4.41
0.3	0.5	0.3	260.32 ± 21.28	0.39 ± 0.10	+24.36 ± 9.37
0.3	1.0	0.3	277.60 ± 32.99	0.36 ± 0.07	+18.71 ± 6.19
0.3	1.5	0.3	310.59 ± 40.03*	0.39 ± 0.10	+28.66 ± 9.19
0.3	2.0	0.3	313.14 ± 29.61*	0.35 ± 0.09	+29.92 ± 5.43

* means significant differences between the value in question and the first formulation ($p<0.05$).

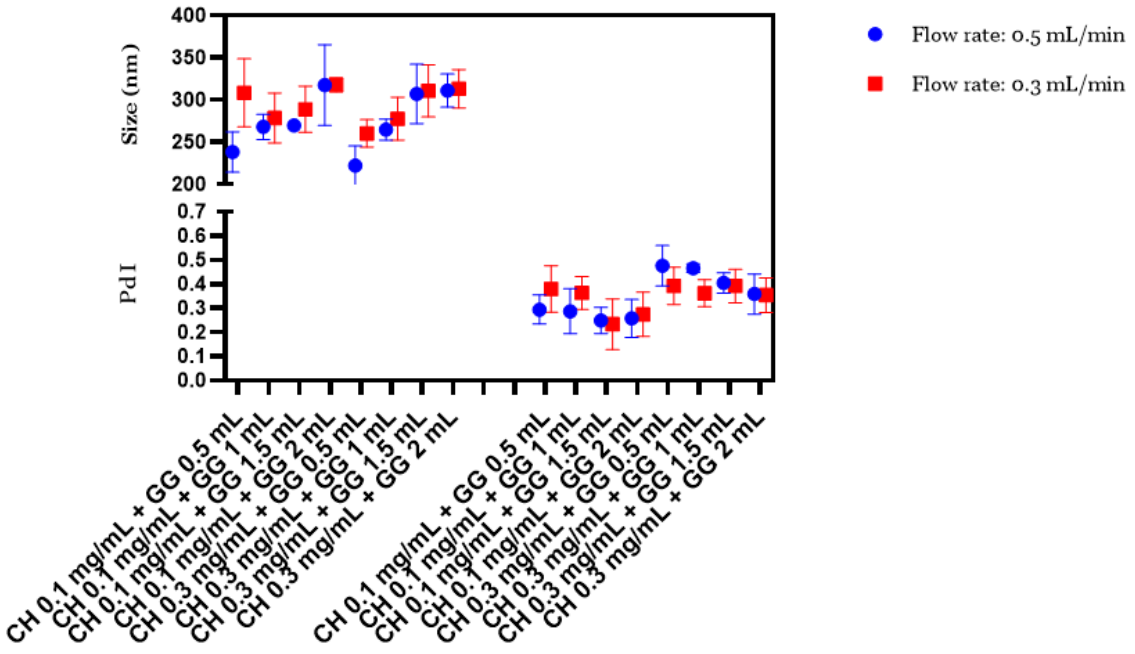

Figure 18 - Size and PdI comparison between the same formulation in different flow rates.

The results showed that an increase in gellan gum volume tend to get bigger NPs, with PdI and zeta potential remaining constant, with few exceptions. This might be due to gellan gum interaction with chitosan, and when gellan gum volume is increased, the

polymer interactions intensify, resulting in the formation of larger delivery systems[120]. An increase in chitosan concentration showed similar NPs in size and in zeta potential but with bigger PdI. This phenomenon can be attributed to the intensified interaction between chitosan molecules itself that can lead to the formation of larger nanoparticle aggregates or clusters within the solution, increasing its heterogeneity[121,122]. Flow rate of 0.5 mL/min revealed slightly smaller NPs with similar PdI and zeta potential when compared to the same formulation but with a flow rate of 0.3 mL/min. At a low flow rate, nanoparticles may have more time to interact and aggregate leading to larger sizes and a broader size distribution. Additionally, slower diffusion rates can result in localized areas of higher polymer concentration, promoting coarsening and non-uniformity in particle size[122,123]. Zeta potential measurements remained similar between the formulations, with few exceptions. The data showed two possible formulations (highlighted in bold) to encapsulate taxifolin with similar sizes and zeta potentials. However, the PdI in the second formulation was statistically significant and bigger than the first one. For that reason, the formulation composed of 0.1 mg/mL of chitosan, 0.5 mL of gellan gum and with a flow rate of 0.5 mL/min was the chosen one to proceed with the plan.

4.2. UV/vis spectrum of CH/GG systems

To examine if the polymers would interact between them and form nanoparticles able to incorporate taxifolin, the UV/vis spectra was traced between 250 and 500 nm[114]. The spectrum is represented in figure 19.

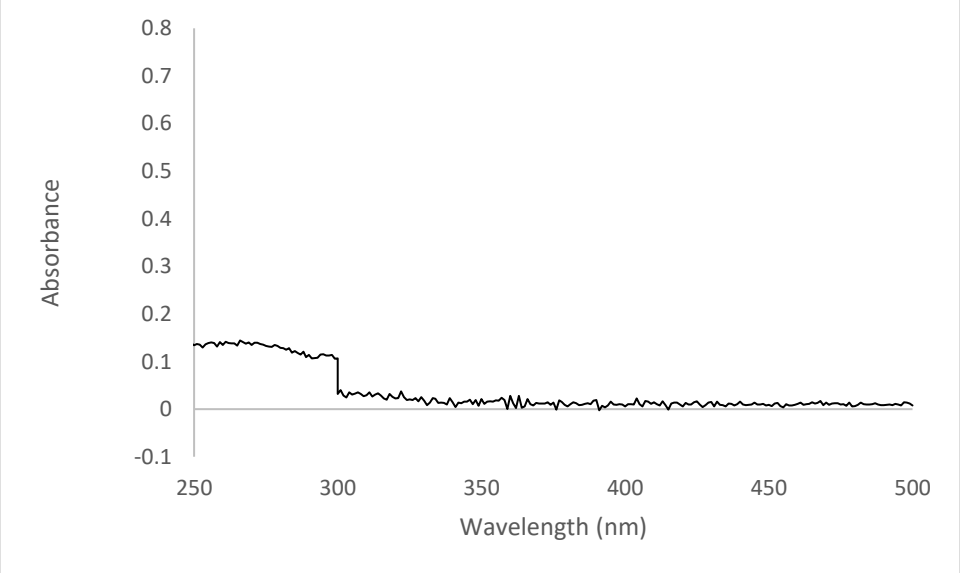

Figure 19 - UV/vis spectrum of CH/GG systems.

The results show that the CH/GG systems have an absorbance value near zero throughout the whole spectra, especially at 289 nm which represents the taxifolin peak[114]. This result indicates that, in further studies, any absorbance value measured at that specific wavelength will be attributed to taxifolin and not to CH/GG systems.

4.3. Development of taxifolin delivery systems

The same formulation technique was used to incorporate the taxifolin into nanoparticles (CH/GG/TAX). In this case, taxifolin was added dropwise to the chitosan solution and then was added the gellan gum solution, also drop by drop. For that, some preliminary studies were performed. First, the taxifolin solubility was tested, being dissolved in 70% ethanol at a concentration of 0.2 mg/mL and in water at concentrations of 0.2 and 0.4 mg/mL, considering its solubility in both solutions. The addition of three different volumes of taxifolin in the formulation was also evaluated (0.1, 0.2 and 0.4 mL) and the results are represented in Table 6.

Table 6- Physico-chemical characterization of CH/GG/TAX formulations obtained by varying the volume of taxifolin solution dissolved in ethanol and water.

Taxifolin dissolved in	Taxifolin concentration (mg/mL)	Taxifolin volume (mL)	Size (nm)	PdI	Zeta Potential (mV)
Ethanol	0.2	0.1	339.24 ± 69.13*	0.38 ± 0.17	+26.00 ± 4.37
		0.2	303.17 ± 31.52*	0.38 ± 0.08	+26.25 ± 5.42
		0.4	390.93 ± 66.11*	0.41 ± 0.11*	+21.47 ± 6.02
Water	0.2	0.1	248.95 ± 22.13	0.35 ± 0.06	+21.40 ± 8.09
		0.2	229.88 ± 23.83	0.34 ± 0.05	+21.14 ± 5.36
		0.4	223.90 ± 24.34	0.32 ± 0.04	+18.65 ± 9.85
	0.4	0.1	296.82 ± 30.58*	0.38 ± 0.09	+30.90 ± 4.14
		0.2	283.36 ± 29.56	0.43 ± 0.04*	+33.12 ± 3.94*
		0.4	276.23 ± 30.68	0.36 ± 0.06	+30.80 ± 5.66
		0.8	450.88 ± 51.13*	0.48 ± 0.08*	+25.75 ± 6.00

* means significant differences between the value in question and the chosen CH/GG formulation ($p<0.05$).

The data demonstrate that nanoparticles formulated with taxifolin dissolved in ethanol presented bigger sizes than when dissolved in water, so the approach of taxifolin dissolved in ethanol was discarded. Between the two different concentrations of taxifolin dissolved in water, as the taxifolin volume increased, the size of delivery systems decreased, except when added 0.8 mL of taxifolin. This can be explained probably because we might be approaching an optimal formulation balance that promotes efficient taxifolin encapsulation while minimizing particle aggregation, resulting in smaller and more consistent nanoparticles[124].

Thus, the formulation approach with 0.4 mg/mL of taxifolin concentration was the chosen one to proceed with further studies, because although the size is slightly

bigger than the formulation made with 0.2 mg/mL of taxifolin, the difference is not statistically significant between those formulations and the CH/GG formulation. Besides, the formulated nanoparticles carry twice the amount of taxifolin which is an asset.

4.4. Fourier transformed infrared spectroscopy

To further ensure that all compounds are present in each one of delivery systems, a FTIR analysis of each isolated polymer as well as CH/GG and CH/GG/TAX formulations was performed. The spectra are present in Figure 20.

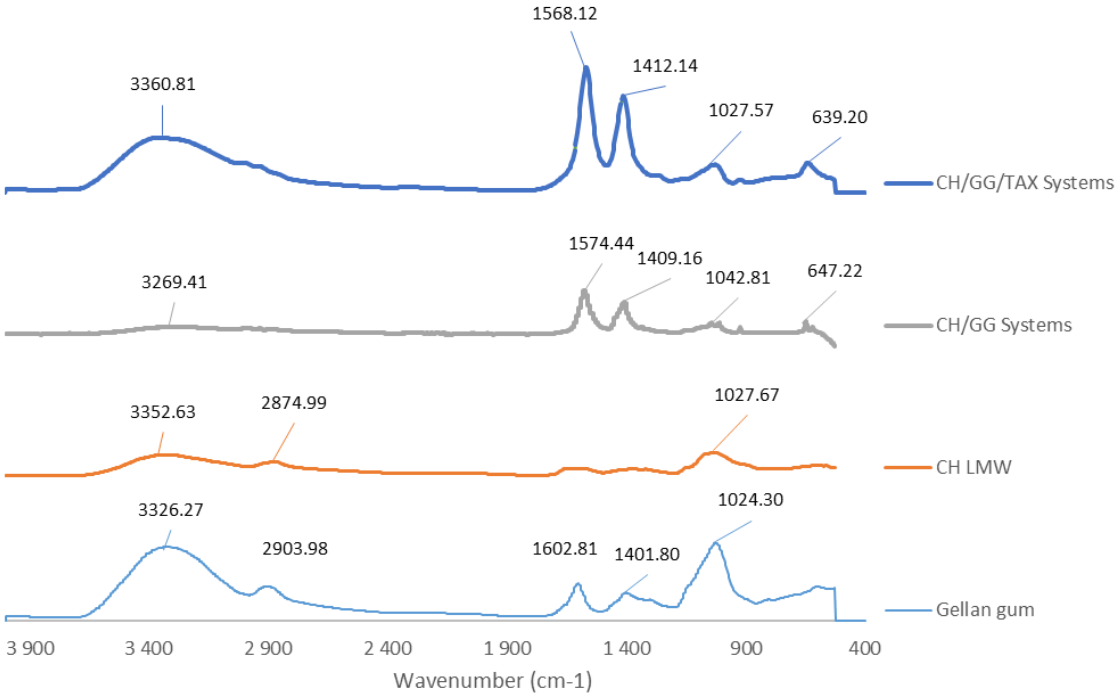

Figure 20 – FTIR spectra of gellan gum, LMW Chitosan, CH/GG systems and CH/GG/TAX systems.

FTIR spectra of LMW chitosan showed a peak at 3352.63 cm^{-1} corresponding to the intermolecular and intramolecular hydrogen bonds -OH and -NH. A characteristic peak at 2874.99 cm^{-1} corresponds to -CH stretching vibrations and the peak at 1027.67 cm^{-1} is attributed to the asymmetric stretching of the C-O-C bridge[125].

Regarding FTIR spectrum of GG, it showed a wide peak at 3326.27 cm^{-1} that can be attributed to the stretching vibrations of -OH, the peak at 2903.98 cm^{-1} corresponds to aliphatic -CH and the peaks at 1602.81, 1401.80 and 1024.30 represents asymmetric COO^-, symmetric COO^- and hydroxylic C-O bonds, respectively[126].

Taxifolin has several characteristics peaks, such as broad peaks in the range of 3300-3500 cm^{-1} corresponding to O-H stretching vibrations; vibrational modes of the aromatic ring C-H bonds can result in peaks in the region of 2900-3100 cm^{-1}; carbonyl group (C=O) typically produces a peak around 1700-1750 cm^{-1}; and carbon-carbon (C-C)

and carbon-oxygen-carbon (C-O-C) result in a fingerprint region (1500-400 cm^{-1}), producing a complex pattern of bands that is unique to the flavonoid structure[127,128].

When the CH/GG systems were analysed, some characteristic peaks were observed of each compound (CH and GG), with slight changes in the wavenumbers of the respective peak that arises from the electrostatic interactions formed between both polymers.

Regarding CH/GG/TAX systems, it is visible an increase of peaks intensity, a shift in the wavenumber and a broader peak at 3360 cm^{-1}. However, it is not visible any characteristic peak of taxifolin, proving that there is no free or unencapsulated taxifolin present in the systems, proving the washing of the sample through centrifugation as previously described works. An increase in peak intensity may be due to the presence of taxifolin, that could indicate changes in the local environment of the functional groups within the nanoparticles. A shift in the wavenumber from 3269 to 3360 cm^{-1} also suggests taxifolin interaction with the polymer matrix. The broadening of peaks implies that there are variations in the local environments and the presence of taxifolin leads to a more complex and diverse molecular environment, through hydrophobic interactions with the hydrophobic sites created by nanoparticles, causing a broadening of peaks. These observations suggest that the incorporation of taxifolin into the nanoparticles has an impact on chemical interactions and, therefore, taxifolin is present in the final formulation.

4.5. Different chitosan types

As mentioned before, initial experiments were made by using LMW chitosan. However, there are different kinds of chitosan with relevance for the pharmaceutical industry. To understand if the type of chitosan used has some influence on the formulated nanoparticles, three different sorts of chitosan were used, namely 5 kDa, LMW and high molecular weight (HMW) chitosans. The main difference between the types of used chitosan is the molecular weight.

Since the most favourable formulation for the incorporation of taxifolin had already been chosen, it made sense to only test the different chitosans with taxifolin already in the systems.

DLS measurements were considered to assess the size, PdI and zeta potential of the nanoparticles and the results are represented in the table 7.

Table 7 - Size and Potential Zeta of nanoparticles with different types of chitosan.

Formulation	Size (nm)	PdI	Zeta potential (mV)
5 kDa CH + GG + TAX	249.00 ± 12.58	0.35 ± 0.10	+17.35 ± 5.64
LMW CH + GG + TAX	276.23 ± 30.68	0.36 ± 0.06	+30.80 ± 5.66
HMW CH + GG + TAX	278.82 ± 53.58	0.33 ± 0.10	+23.59 ± 5.94

Nanoparticles formulated with LMW and HMW chitosans showed very similar results in terms of size, PdI and zeta potential between them. The data also show that nanoparticles formulated with 5 kDa chitosan were smaller and had less zeta potential when compared to other types of chitosan. This can be explained due to the shorter polymer chains that present fewer charged groups and could lead to smaller-sized nanoparticles[129]. However, further characterization studies were made using these three kinds of chitosan to fully understand the influence of each chitosan in the previous formulation.

4.6. Scanning electron microscopy

The morphology of delivery systems can also influence cellular internalization, making this parameter of high relevance to verify if the delivery systems have a regular, uniform and spherical shape[130]. In this sense, SEM was performed for both CH/GG and CH/GG/TAX systems to assess the morphology of the nanoparticles and the results are displayed in Figure 21.

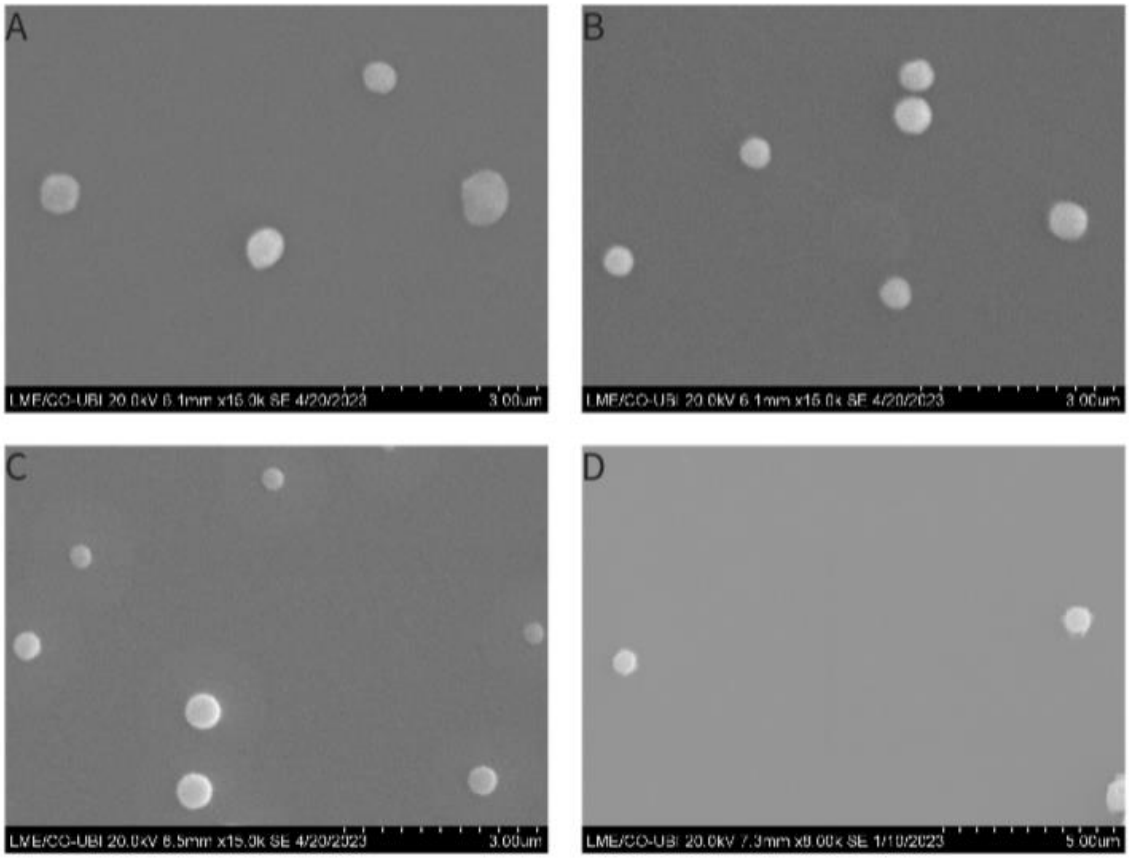

Figure 21 - SEM images: (**A**) CH/GG systems, (**B**) 5 kDa CH/GG/TAX systems, (**C**) LMW CH/GG/TAX, (**D**), HMW CH/GG/TAX systems.

According to SEM results, all the nanoparticles showed spherical and uniform shapes, independently of the chitosan used, making it ideal to a posterior cell

delivery[131]. However, nanoparticles formulated with LMW chitosan seem to be the most uniform between all the systems tested.

4.7. Encapsulation efficiency

Encapsulation efficiency can be defined as the percentage of drug that is successfully entrapped into the micelle or nanoparticle and it is influenced by various factors, with the interaction between the drug's hydrophobic nature and the hydrophobic regions of the delivery system being particularly significant[132].

Thus, to determine the amount of taxifolin incorporated into the delivery systems with different CH, the amount of free taxifolin was measured using the HPLC technique. The obtained results are showed in Table 8.

Table 8 - Encapsulation efficiency of each delivery system.

Delivery system	EE (%)
5 kDa CH NPs	53.52 ± 6.56
LMW CH NPs	65.56 ± 5.80
HMW CH NPs	53.69 ± 4.47

The results obtained by HPLC showed nanoparticles made with 5 kDa and HMW chitosan encapsulated around 54% and delivery systems made with LMW chitosan showed good encapsulation efficiency, with around 66%. Some possible reasons for this are that nanoparticles formulated with 5 kDa chitosan did not provided enough chain length for favourable interaction, whereas HMW chitosan, due to its longer polymer chains, resulted in less surface area providing fewer active sites for taxifolin interaction. LMW chitosan showed a good balance between an enough chain length and an adequate surface area for taxifolin encapsulation[129,133]. These encapsulation efficiency values are satisfactory, since flavonoids encapsulation through polymer nanoparticles typically present encapsulation efficiencies between 19 and 80%[134,135]

4.8. *In vitro* release studies

To monitor taxifolin release profile from the delivery systems formulated with different CH types, release studies were performed over 3 days. Release studies were performed at two different pH to mimic some conditions in the human body. These assays were performed at pH 7.4, which represents the normal bloodstream pH and at pH 5.8, representative of the pH found in a tumoral environment[136]. The data obtained is presented in Figure 22.

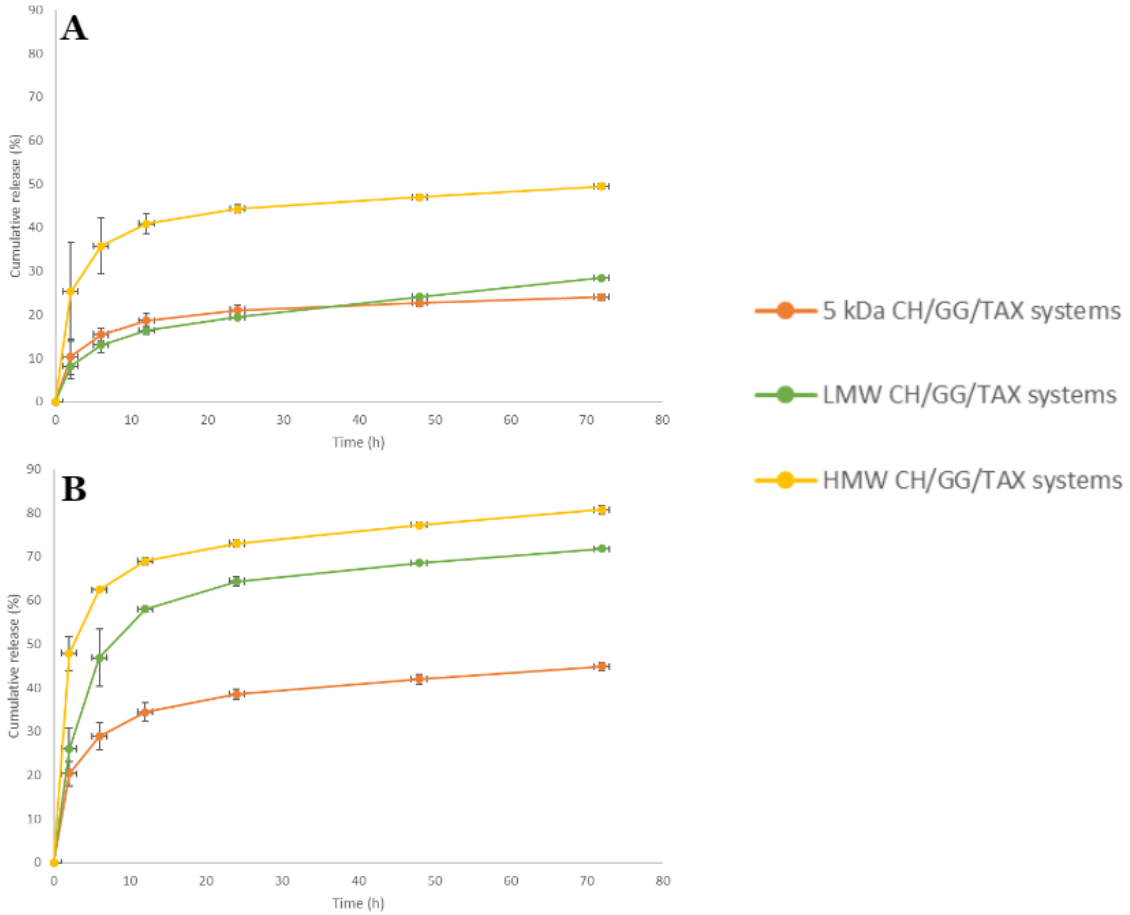

Figure 22 - *In vitro* release studies: (**A**) pH 7.4, (**B**) pH 5.8.

The results show that every system sustained a controlled release that can be associated to the diffusion or time-dependent degradation of delivery systems.

However, ideally, there should be low taxifolin release at pH 7.4, which indicates that the delivery systems are stable during the passage in the bloodstream. When the systems arrive at the tumoral site, where an acidic pH is present, a significant taxifolin release should be obtained, thereby targeting these delivery systems to cancer cells[136,137]. The results show that 5k Da CH/GG/TAX systems presented a reasonable releasing profile at pH 7.4 but poorly released at pH 5.8. Between the two remaining systems, HMW CH/GG/TAX showed high releasing profile at both pH studied, while LMW CH/GG/TAX systems revealed low release at pH 7.4 and a high release at pH 5.8. The release behaviour of the LMW CH/GG/TAX suggests this system can be adequate to deliver the taxifolin in the tumour environment and avoid its lost in systemic circulation.

Overall, and considering all obtained results, LMW CH/GG/TAX systems were the ones that showed best morphology, best encapsulation efficiency and better releasing profiles and, for these reasons, the remaining systems were discarded and LMW CH/GG/TAX were the only ones that proceeded to the cellular assays.

4.9. Delivery systems internalization studies

HeLa and hFiB cell lines were used to evaluate the capability for cell uptake and internalization by the delivery systems. The images of the internalization studies are presented in Figures 23 and 24, with the nuclei stained blue with DAPI and the chitosan of delivery systems are stained green with FITC.

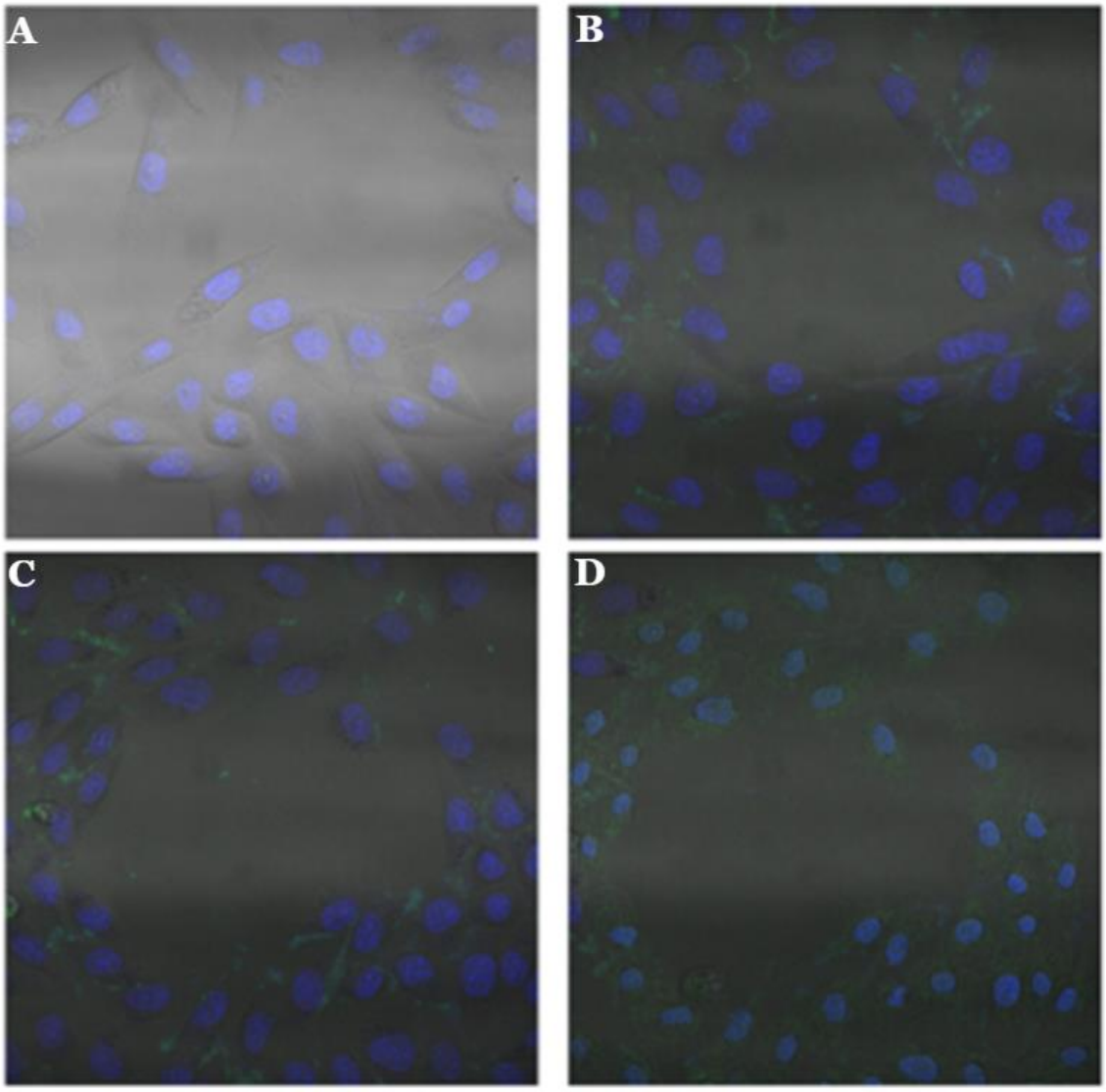

Figure 23 - Uptake of FITC labelled LMW CH/GG/TAX delivery systems in HeLa cells: (**A**) control group (non-treated), (**B**) after 2 h of incubation, (**C**) after 4 h of incubation, (**D**) after 6 h of incubation.

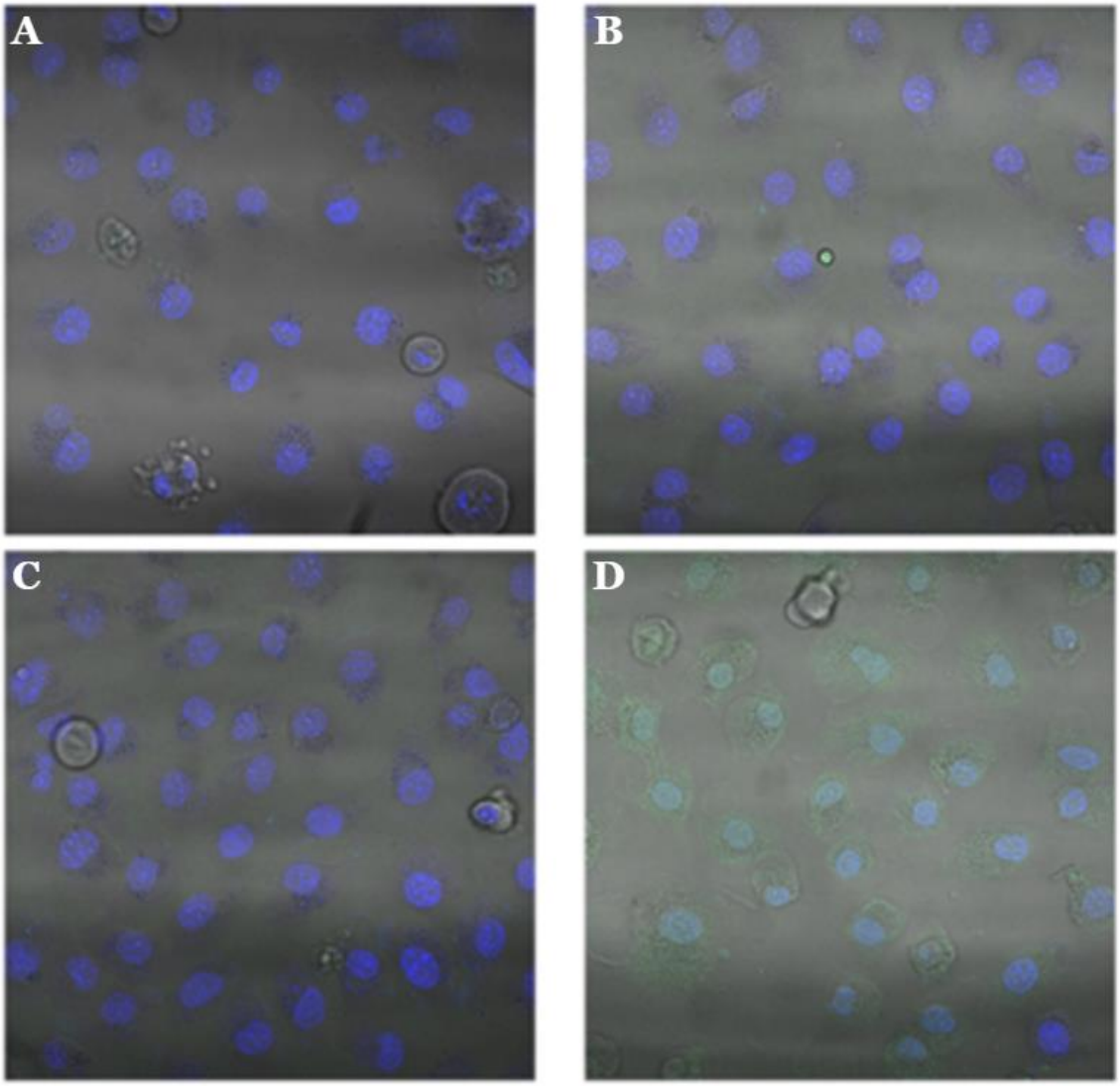

Figure 24 - Uptake of FITC labelled LMW CH/GG/TAX delivery systems in hFiB cells: (**A**) control group (non-treated), (**B**) after 2 h of incubation, (**C**) after 4 h of incubation, (**D**) after 6 h of incubation.

Figures 22 and 23 show that after 2 h, some delivery systems are dispersed in the medium while other nanoparticles are in the surroundings of both cell lines, after 4 h some delivery systems have already entered the cells and after 6 h it is possible to observe that most delivery systems have entered both HeLa and hFiB cell lines.

These results indicate these systems present a good internalization efficiency in both cell lines. However, we expect to observe a taxifolin therapeutic effect only in HeLa cells due to the specific action of this molecule in the HPV E6 oncoprotein inhibition. With an increase in taxifolin concentration, it is anticipated that there will be an impact on the viability of HPV-positive cells through a blockade of E6 recognition by the p53 protein that will result in the restoration of levels of this tumor suppressor protein, inducing apoptosis in HeLa cells.

However, according to expected and described previously, more studies need to be carried out, such as viability studies, IC_{50} determination, western blot to assess the

levels of p53, Bax or other intervenient of the apoptotic pathway, to fully understand the effectiveness of these systems.

5. Conclusions and future perspectives

Cervical cancer incidence and mortality have been declining, but it remains a leading cause of death in less developed nations where anti-HPV preventative immunizations are not widely used and health care is inadequate. With this in mind, treatments for HPV infections and cervical cancer have been researched. Taxifolin, one of the most promising flavonoids, has emerged as a molecule with demonstrated anti-cancer potency. Taxifolin, in addition to its anti-cancer capabilities, has the ability to block the E6 oncoprotein, which increases p53 levels and induces apoptosis. Nonetheless, the vast majority of flavonoids, such as taxifolin, have relatively low bioavailability due to poor water solubility, easy degradation and fast metabolism.

Thus, it is imperative to study ways to encapsulate this type of drugs and ensure its controlled delivery to cancer cells.

The aim of this work was the development of taxifolin loaded delivery systems to be applied in HPV positive cells, aiming to increase the effect of taxifolin. For this purpose, three types of delivery systems were formulated and characterized, being them formulated with different types of chitosan, gellan gum and taxifolin (CH/GG/TAX systems). The ratios have been optimized in order to obtain the most favourable delivery systems in terms of size, PdI and surface charge.

Hence, it was possible to obtain optimised delivery systems of LMW CH/GG/TAX with a size of 276.23 ± 30.68 nm, a PdI of 0.36 ± 0.06 and a zeta potential of +30.80 ± 5.66 mV, delivery systems of 5 kDa CH/GG/TAX with a size of 249.00 ± 12.58 nm, a PdI of 0.35 ± 0.10 and a zeta potential of +17.35 ± 5.64 mV and delivery systems of HMW CH/GG/TAX with a size of 278.82 ± 53.58 nm, a PdI of 0.33 ± 0.10 and a zeta potential of +23.59 ± 5.94 mV. After that, the encapsulation efficiency of taxifolin in the delivery systems was calculated, being the formulation made with LMW CH/GG/TAX the most favorable, reaching 65% of encapsulation, while the other formulations encapsulated around 55%.

Furthermore, all systems were characterized in their morphology by SEM and in interactions between their components by FTIR. The results showed spherical delivery systems and FTIR analysis revealed interactions between all the components in all delivery systems.

In vitro release studies were also performed to analyse the amount of taxifolin that the systems released during 72 h and if the release occurred in a controlled manner under two different pHs, representing a tumor microenvironment (pH 5.8) and the bloodstream (pH 7.4). Results showed that delivery systems made with LMW CH/GG/TAX systems presented the best releasing profiles, based on a good release at pH 5.8 (72%) and a low release at pH 7.4(28%).

Cell internalization studies revealed that LMWCH/GG/TAX systems were able to successfully enter the cells.

As future perspectives, other studies can be carried out, such as cell viability studies and quantification of p53 levels in order to ensure that the delivery systems present an increase in the expression levels of p53, indicating an inhibition of the carcinogenesis processes and apoptosis induction. Moreover, studies in co-culture may be addressed to mimic more closely cellular interactions and better simulate tissue microenvironments to test the performance of these delivery systems.

Modifications in the delivery systems preparation can also be made, such as lyophilisation of the systems after their formulation, as well the inclusion of specific ligands to specifically direct them to the cancer cells, thus enabling a greater therapeutic effect.

This work had an important exploratory nature in determining the optimal formulation of taxifolin delivery systems through the combination of two natural polymers with opposing charges. It evaluated the physicochemical properties and characteristics of the systems, as well as their capacity to incorporate and release taxifolin. This information is crucial for advancing towards therapeutic applications of taxifolin or other potential pharmaceuticals.

References

[1] https://gco.iarc.fr/today/data/factsheets/cancers/39-All-cancers-fact-sheet.pdf n.d.

[2] Roy PS, Saikia BJ. Cancer and cure: A critical analysis. Indian J Cancer 2016;53:441–2. https://doi.org/10.4103/0019-509X.200658.

[3] Hanahan D, Weinberg RA. Hallmarks of cancer: the next generation. Cell 2011;144:646–74. https://doi.org/10.1016/J.CELL.2011.02.013.

[4] Cancer n.d. https://www.who.int/news-room/fact-sheets/detail/cancer (accessed May 8, 2023).

[5] Hausman DM. What is cancer? Perspect Biol Med 2019;62:778–84. https://doi.org/10.1353/PBM.2019.0046.

[6] Szymonowicz KA, Chen J. Biological and clinical aspects of HPV-related cancers. Cancer Biol Med 2020;17:864–78. https://doi.org/10.20892/j.issn.2095-3941.2020.0370.

[7] Bray F, Ferlay J, Soerjomataram I, Siegel RL, Torre LA, Jemal A. Global cancer statistics 2018: GLOBOCAN estimates of incidence and mortality worldwide for 36 cancers in 185 countries. CA Cancer J Clin 2018;68:394–424. https://doi.org/10.3322/caac.21492.

[8] Almeida AM, Queiroz JA, Sousa F, Sousa Â. Cervical cancer and HPV infection: ongoing therapeutic research to counteract the action of E6 and E7 oncoproteins. Drug Discov Today 2019;24:2044–57. https://doi.org/10.1016/J.DRUDIS.2019.07.011.

[9] Satterwhite CL, Torrone E, Meites E, Dunne EF, Mahajan R, Cheryl Bañez Ocfemia M, et al. Sexually transmitted infections among US women and men: Prevalence and incidence estimates, 2008. Sex Transm Dis 2013;40:187–93. https://doi.org/10.1097/OLQ.0B013E318286BB53.

[10] Koutsky L. Epidemiology of Genital Human Papillomavirus Infection. Am J Med 1997;102:3–8. https://doi.org/10.1016/S0002-9343(97)00177-0.

[11] Van Doorslaer K, Tan Q, Xirasagar S, Bandaru S, Gopalan V, Mohamoud Y, et al. The Papillomavirus Episteme: a central resource for papillomavirus sequence data and analysis. Nucleic Acids Res 2013;41:D571. https://doi.org/10.1093/NAR/GKS984.

[12] De Villiers EM, Fauquet C, Broker TR, Bernard HU, Zur Hausen H. Classification of papillomaviruses. Virology 2004;324:17–27. https://doi.org/10.1016/J.VIROL.2004.03.033.

[13] Sak K. Characteristic features of cytotoxic activity of flavonoids on human cervical cancer cells. Asian Pacific Journal of Cancer Prevention 2014;15:8007–19. https://doi.org/10.7314/APJCP.2014.15.19.8007.

[14] Graham S V. Human papillomavirus: gene expression, regulation and prospects for novel diagnostic methods and antiviral therapies. Future Microbiol 2010;5:1493. https://doi.org/10.2217/FMB.10.107.

[15] Herfs M, Yamamoto Y, Laury A, Wang X, Nucci MR, McLaughlin-Drubin ME, et al. A discrete population of squamocolumnar junction cells implicated in the pathogenesis of cervical cancer. Proc Natl Acad Sci U S A 2012;109:10516–21. https://doi.org/10.1073/PNAS.1202684109/-/DCSUPPLEMENTAL.

[16] Balasubramaniam SD, Balakrishnan V, Oon CE, Kaur G. Key Molecular Events in Cervical Cancer Development. Medicina (B Aires) 2019;55. https://doi.org/10.3390/MEDICINA55070384.

[17] Choi YJ, Park JS. Clinical significance of human papillomavirus genotyping. J Gynecol Oncol 2016;27. https://doi.org/10.3802/JGO.2016.27.E21.

[18] Westrich JA, Warren CJ, Pyeon D. Evasion of Host Immune Defenses by Human Papillomavirus. Virus Res 2017;231:21. https://doi.org/10.1016/J.VIRUSRES.2016.11.023.

[19] Oldak M, Smola H, Aumailley M, Rivero F, Pfister H, Smola-Hess S. The Human Papillomavirus Type 8 E2 Protein Suppresses β4-Integrin Expression in Primary Human Keratinocytes. J Virol 2004;78:10738. https://doi.org/10.1128/JVI.78.19.10738-10746.2004.

[20] Hoppe-Seyler K, Bossler F, Braun JA, Herrmann AL, Hoppe-Seyler F. The HPV E6/E7 Oncogenes: Key Factors for Viral Carcinogenesis and Therapeutic Targets. Trends Microbiol 2018;26:158–68. https://doi.org/10.1016/J.TIM.2017.07.007.

[21] Moody CA, Laimins LA. Human papillomavirus oncoproteins: pathways to transformation. Nature Reviews Cancer 2010 10:8 2010;10:550–60. https://doi.org/10.1038/nrc2886.

[22] Graham S V. The human papillomavirus replication cycle, and its links to cancer progression: a comprehensive review. Clin Sci 2017;131:2201–21. https://doi.org/10.1042/CS20160786.

[23] Thomas M, David P, Banks L. The role of the E6-p53 interaction in the molecular pathogenesis of HPV. Oncogene 1999;18:7690–700. https://doi.org/10.1038/SJ.ONC.1202953.

[24] Franconi R, Massa S, Paolini F, Vici P, Venuti A. Plant-Derived Natural Compounds in Genetic Vaccination and Therapy for HPV-Associated Cancers.

Cancers 2020, Vol 12, Page 3101 2020;12:3101. https://doi.org/10.3390/CANCERS12113101.

[25] Almeida AM, Queiroz JA, Sousa F, Sousa Â. Cervical cancer and HPV infection: ongoing therapeutic research to counteract the action of E6 and E7 oncoproteins. Drug Discov Today 2019;24:2044–57. https://doi.org/10.1016/J.DRUDIS.2019.07.011.

[26] Hofstetter AM, Rosenthal SL. Factors impacting HPV vaccination: Lessons for health care professionals. Expert Rev Vaccines 2014;13:1013–26. https://doi.org/10.1586/14760584.2014.933076.

[27] Gomes D, Yaduvanshi S, Silvestre S, Duarte AP, Santos AO, Soares CP, et al. Taxifolin and Lucidin as Potential E6 Protein Inhibitors: p53 Function Re-Establishment and Apoptosis Induction in Cervical Cancer Cells. Cancers (Basel) 2022;14. https://doi.org/10.3390/cancers14122834.

[28] Panche AN, Diwan AD, Chandra SR. Flavonoids: an overview. J Nutr Sci 2016;5:e47. https://doi.org/10.1017/JNS.2016.41.

[29] Kopustinskiene DM, Jakstas V, Savickas A, Bernatoniene J. Flavonoids as Anticancer Agents. Nutrients 2020, Vol 12, Page 457 2020;12:457. https://doi.org/10.3390/NU12020457.

[30] Liu J, Wang X, Yong H, Kan J, Jin C. Recent advances in flavonoid-grafted polysaccharides: Synthesis, structural characterization, bioactivities and potential applications. Int J Biol Macromol 2018;116:1011–25. https://doi.org/10.1016/J.IJBIOMAC.2018.05.149.

[31] Rodríguez-García C, Sánchez-Quesada C, Gaforio JJ, Gaforio JJ. Dietary Flavonoids as Cancer Chemopreventive Agents: An Updated Review of Human Studies. Antioxidants 2019, Vol 8, Page 137 2019;8:137. https://doi.org/10.3390/ANTIOX8050137.

[32] Murphy MP. How mitochondria produce reactive oxygen species. Biochemical Journal 2009;417:1–13. https://doi.org/10.1042/BJ20081386.

[33] Ferreira M, Costa D, Sousa Â. Flavonoids-Based Delivery Systems towards Cancer Therapies. Bioengineering 2022, Vol 9, Page 197 2022;9:197. https://doi.org/10.3390/BIOENGINEERING9050197.

[34] Gomes D, Silvestre S, Duarte AP, Venuti A, Soares CP, Passarinha L, et al. pharmaceuticals In Silico Approaches: A Way to Unveil Novel Therapeutic Drugs for Cervical Cancer Management 2021. https://doi.org/10.3390/ph14080741.

[35] Navarro-Hortal MD, Varela-López A, Romero-Márquez JM, Rivas-García L, Speranza L, Battino M, et al. Role of flavonoids against adriamycin toxicity. Food Chem Toxicol 2020;146. https://doi.org/10.1016/J.FCT.2020.111820.

[36] Seleem D, Pardi V, Murata RM. Review of flavonoids: A diverse group of natural compounds with anti-Candida albicans activity in vitro. Arch Oral Biol 2017;76:76–83. https://doi.org/10.1016/J.ARCHORALBIO.2016.08.030.

[37] Clemente-Soto AF, Salas-Vidal E, Milan-Pacheco C, Sánchez-Carranza JN, Peralta-Zaragoza O, González-Maya L. Quercetin induces G2 phase arrest and apoptosis with the activation of p53 in an E6 expression-independent manner in HPV-positive human cervical cancer-derived cells. Mol Med Rep 2019;19:2097–106. https://doi.org/10.3892/MMR.2019.9850.

[38] Seleem D, Pardi V, Murata RM. Review of flavonoids: A diverse group of natural compounds with anti-Candida albicans activity in vitro. Arch Oral Biol 2017;76:76–83. https://doi.org/10.1016/J.ARCHORALBIO.2016.08.030.

[39] Hsiao YC, Kuo WH, Chen PN, Chang HR, Lin TH, Yang WE, et al. Flavanone and 2′-OH flavanone inhibit metastasis of lung cancer cells via down-regulation of proteinases activities and MAPK pathway. Chem Biol Interact 2007;167:193–206. https://doi.org/10.1016/J.CBI.2007.02.012.

[40] Shen N, Wang T, Gan Q, Liu S, Wang L, Jin B. Plant flavonoids: Classification, distribution, biosynthesis, and antioxidant activity. Food Chem 2022;383:132531. https://doi.org/10.1016/J.FOODCHEM.2022.132531.

[41] Almasoudi HH, Hakami MA, Alhazmi AY, Makkawi M, Alasmari S, Alghamdi YS, et al. Unveiling the multitargeted repurposing potential of taxifolin (dihydroquercetin) in cervical cancer: an extensive MM\GBSA-based screening, and MD simulation study. Medical Oncology 2023;40:1–15. https://doi.org/10.1007/S12032-023-02094-7/FIGURES/7.

[42] Heiss C, Keen CL, Kelm M. Flavanols and cardiovascular disease prevention. Eur Heart J 2010;31:2583–92. https://doi.org/10.1093/EURHEARTJ/EHQ332.

[43] Hong T, Ham J, Song G, Lim W. Alpinumisoflavone Disrupts Endoplasmic Reticulum and Mitochondria Leading to Apoptosis in Human Ovarian Cancer. Pharmaceutics 2022;14. https://doi.org/10.3390/PHARMACEUTICS14030564.

[44] Cahyana Y, Adiyanti T. Flavonoids as Antidiabetic Agents. Indonesian Journal of Chemistry 2021;21:512–26. https://doi.org/10.22146/IJC.58439.

[45] Ferreira MKA, Fontenelle ROS, Magalhães FEA, Bandeira PN, De Menezes JSEA, Dos Santos HS. Chalcones pharmacological potential: A brief review. Revista Virtual de Quimica 2018;10:1455–73. https://doi.org/10.21577/1984-6835.20180099.

[46] A REVIEW ON NATURAL CHALCONES AN UPDATE | INTERNATIONAL JOURNAL OF PHARMACEUTICAL SCIENCES AND RESEARCH n.d.

https://ijpsr.com/bft-article/a-review-on-natural-chalcones-an-update/ (accessed September 5, 2023).

[47] Sinopoli A, Calogero G, Bartolotta A. Computational aspects of anthocyanidins and anthocyanins: A review. Food Chem 2019;297:124898. https://doi.org/10.1016/J.FOODCHEM.2019.05.172.

[48] Thilakarathna SH, Vasantha Rupasinghe HP. Flavonoid Bioavailability and Attempts for Bioavailability Enhancement. Nutrients 2013;5:3367. https://doi.org/10.3390/NU5093367.

[49] Yousefi M, Shadnoush M, Sohrabvandi S, Khorshidian N, Mortazavian AM. Encapsulation Systems for Delivery of Flavonoids: A Review 2021;11:13934–51. https://doi.org/10.33263/BRIAC116.1393413951.

[50] Khan H, Ullah H, Martorell M, Valdes SE, Belwal T, Tejada S, et al. Flavonoids nanoparticles in cancer: Treatment, prevention and clinical prospects. Semin Cancer Biol 2021;69:200–11. https://doi.org/10.1016/J.SEMCANCER.2019.07.023.

[51] dos Santos Lima B, Shanmugam S, de Souza Siqueira Quintans J, Quintans-Júnior LJ, de Souza Araújo AA. Inclusion complex with cyclodextrins enhances the bioavailability of flavonoid compounds: a systematic review. Phytochemistry Reviews 2019;5:1337–59. https://doi.org/10.1007/S11101-019-09650-Y.

[52] Li J, Shi M, Ma B, Niu R, Zhang H, Kun L. Antitumor activity and safety evaluation of nanaparticle-based delivery of quercetin through intravenous administration in mice. Materials Science and Engineering: C 2017;77:803–10. https://doi.org/10.1016/J.MSEC.2017.03.191.

[53] Li J, Li Z, Gao Y, Liu S, Li K, Wang S, et al. Effect of a Drug Delivery System Made of Quercetin Formulated into PEGylation Liposomes on Cervical Carcinoma in Vitro and in Vivo. J Nanomater 2021;2021. https://doi.org/10.1155/2021/9389934.

[54] Saraswat AL, Maher TJ. Development and optimization of stealth liposomal system for enhanced in vitro cytotoxic effect of quercetin. J Drug Deliv Sci Technol 2020;55. https://doi.org/10.1016/J.JDDST.2019.101477.

[55] Dora CL, Silva LFC, Mazzarino L, Siqueira JM, Fernandes D, Pacheco LK, et al. Oral Delivery of a High Quercetin Payload Nanosized Emulsion: In Vitro and In Vivo Activity Against B16-F10 Melanoma. J Nanosci Nanotechnol 2016;16:1275–81. https://doi.org/10.1166/JNN.2016.11675.

[56] Ni S, Hu C, Sun R, Zhao G, Xia Q. Nanoemulsions-Based Delivery Systems for Encapsulation of Quercetin: Preparation, Characterization, and Cytotoxicity Studies. J Food Process Eng 2017;40. https://doi.org/10.1111/JFPE.12374.

[57] Bhia M, Motallebi M, Abadi B, Zarepour A, Pereira-Silva M, Saremnejad F, et al. Naringenin Nano-Delivery Systems and Their Therapeutic Applications. Pharmaceutics 2021;13:1–29. https://doi.org/10.3390/PHARMACEUTICS13020291.

[58] Bose S, Du Y, Takhistov P, Michniak-Kohn B. Formulation optimization and topical delivery of quercetin from solid lipid based nanosystems. Int J Pharm 2013;441:56–66. https://doi.org/10.1016/J.IJPHARM.2012.12.013.

[59] Scalia S, Haghi M, Losi V, Trotta V, Young PM, Traini D. Quercetin solid lipid microparticles: A flavonoid for inhalation lung delivery. European Journal of Pharmaceutical Sciences 2013;49:278. https://doi.org/10.1016/J.EJPS.2013.03.009.

[60] Zu Y, Wu W, Zhao X, Li Y, Wang W, Zhong C, et al. Enhancement of solubility, antioxidant ability and bioavailability of taxifolin nanoparticles by liquid antisolvent precipitation technique. Int J Pharm 2014;471:366–76. https://doi.org/10.1016/j.ijpharm.2014.05.049.

[61] Deepika MS, Thangam R, Sheena TS, Sasirekha R, Sivasubramanian S, Babu MD, et al. A novel rutin-fucoidan complex based phytotherapy for cervical cancer through achieving enhanced bioavailability and cancer cell apoptosis. Biomedicine & Pharmacotherapy 2019;109:1181–95. https://doi.org/10.1016/J.BIOPHA.2018.10.178.

[62] Wang W, Sun C, Mao L, Ma P, Liu F, Yang J, et al. The biological activities, chemical stability, metabolism and delivery systems of quercetin: A review. Trends Food Sci Technol 2016;56:21–38. https://doi.org/10.1016/J.TIFS.2016.07.004.

[63] Zhang X, Xu M, Zhang Z, Hu X, Hao L, Lin Q, et al. Preparation and characterization of magnetic fluorescent microspheres for delivery of kaempferol. Http://DxDoiOrg/101080/1066785720161157913 2016;32:125–30. https://doi.org/10.1080/10667857.2016.1157913.

[64] Rahimi S, Khoee S, Ghandi M. Preparation and characterization of rod-like chitosan–quinoline nanoparticles as pH-responsive nanocarriers for quercetin delivery. Int J Biol Macromol 2019;128:279–89. https://doi.org/10.1016/J.IJBIOMAC.2019.01.137.

[65] Filho IK, Machado CS, Diedrich C, Karam TK, Nakamura CV, Khalil NM, et al. Optimized Chitosan-Coated Gliadin Nanoparticles Improved the Hesperidin Cytotoxicity over Tumor Cells. Brazilian Archives of Biology and Technology 2021;64:e21200795. https://doi.org/10.1590/1678-4324-75YEARS-2021200795.

[66] Yamina AM, Fizir M, Itatahine A, He H, Dramou P. Preparation of multifunctional PEG-graft-Halloysite Nanotubes for Controlled Drug Release, Tumor Cell Targeting, and Bio-imaging. Colloids Surf B Biointerfaces 2018;170:322–9. https://doi.org/10.1016/J.COLSURFB.2018.06.042.

[67] El-Gogary RI, Rubio N, Wang JTW, Al-Jamal WT, Bourgognon M, Kafa H, et al. Polyethylene glycol conjugated polymeric nanocapsules for targeted delivery of quercetin to folate-expressing cancer cells in vitro and in vivo. ACS Nano 2014;8:1384–401. https://doi.org/10.1021/NN405155B.

[68] Tymon-Rosario J, Zeybek B, Santin AD. Novel antibody-drug conjugates: current and future roles in gynecologic oncology. Curr Opin Obstet Gynecol 2021;33:26–33. https://doi.org/10.1097/GCO.0000000000000642.

[69] Yamina AM, Fizir M, Itatahine A, He H, Dramou P. Preparation of multifunctional PEG-graft-Halloysite Nanotubes for Controlled Drug Release, Tumor Cell Targeting, and Bio-imaging. Colloids Surf B Biointerfaces 2018;170:322–9. https://doi.org/10.1016/J.COLSURFB.2018.06.042.

[70] Krauland AH, Alonso MJ. Chitosan/cyclodextrin nanoparticles as macromolecular drug delivery system. Int J Pharm 2007;340:134–42. https://doi.org/10.1016/J.IJPHARM.2007.03.005.

[71] Mashhadi Malekzadeh A, Ramazani A, Tabatabaei Rezaei SJ, Niknejad H. Design and construction of multifunctional hyperbranched polymers coated magnetite nanoparticles for both targeting magnetic resonance imaging and cancer therapy. J Colloid Interface Sci 2017;490:64–73. https://doi.org/10.1016/J.JCIS.2016.11.014.

[72] Kim ES, Kim DY, Lee JS, Lee HG. Quercetin delivery characteristics of chitosan nanoparticles prepared with different molecular weight polyanion cross-linkers. Carbohydr Polym 2021;267:118157. https://doi.org/10.1016/J.CARBPOL.2021.118157.

[73] Wan Z, Zheng R, Moharil P, Liu Y, Chen J, Sun R, et al. Polymeric Micelles in Cancer Immunotherapy. Molecules 2021;26:1220. https://doi.org/10.3390/MOLECULES26051220.

[74] Stan D, Enciu AM, Mateescu AL, Ion AC, Brezeanu AC, Stan D, et al. Natural Compounds With Antimicrobial and Antiviral Effect and Nanocarriers Used for Their Transportation. Front Pharmacol 2021;12:723233. https://doi.org/10.3389/FPHAR.2021.723233.

[75] Chen LC, Chen YC, Su CY, Hong CS, Ho HO, Sheu MT. Development and characterization of self-assembling lecithin-based mixed polymeric micelles

containing quercetin in cancer treatment and an in vivo pharmacokinetic study. Int J Nanomedicine 2016;11:1557. https://doi.org/10.2147/IJN.S103681.

[76] Löf D, Schillén K, Nilsson L. Flavonoids: Precipitation Kinetics and Interaction with Surfactant Micelles. J Food Sci 2011;76:N35–9. https://doi.org/10.1111/J.1750-3841.2011.02103.X.

[77] Perumal S, Atchudan R, Lee W. A Review of Polymeric Micelles and Their Applications. Polymers 2022, Vol 14, Page 2510 2022;14:2510. https://doi.org/10.3390/POLYM14122510.

[78] Suvarna V, Bore B, Bhawar C, Mallya R. Complexation of phytochemicals with cyclodextrins and their derivatives- an update. Biomedicine & Pharmacotherapy 2022;149:112862. https://doi.org/10.1016/J.BIOPHA.2022.112862.

[79] Pinho E, Grootveld M, Soares G, Henriques M. Cyclodextrins as encapsulation agents for plant bioactive compounds. Carbohydr Polym 2014;101:121–35. https://doi.org/10.1016/J.CARBPOL.2013.08.078.

[80] Suvarna V, Gujar P, Murahari M. Complexation of phytochemicals with cyclodextrin derivatives – An insight. Biomedicine & Pharmacotherapy 2017;88:1122–44. https://doi.org/10.1016/J.BIOPHA.2017.01.157.

[81] Ferreira M, Gomes D, Neto M, Passarinha LA, Costa D, Sousa Â. Development and Characterization of Quercetin-Loaded Delivery Systems for Increasing Its Bioavailability in Cervical Cancer Cells. Pharmaceutics 2023;15. https://doi.org/10.3390/PHARMACEUTICS15030936.

[82] Yang J, Li K, He D, Gu J, Xu J, Xie J, et al. Toward a better understanding of metabolic and pharmacokinetic characteristics of low-solubility, low-permeability natural medicines. Https://DoiOrg/101080/0360253220201714646 2020;52:19–43. https://doi.org/10.1080/03602532.2020.1714646.

[83] Dias AP, da Silva Santos S, da Silva JV, Parise-Filho R, Igne Ferreira E, Seoud O El, et al. Dendrimers in the context of nanomedicine. Int J Pharm 2020;573:118814. https://doi.org/10.1016/J.IJPHARM.2019.118814.

[84] Singh A, Id C. Dendrimers for Drug Delivery. Molecules 2018, Vol 23, Page 938 2018;23:938. https://doi.org/10.3390/MOLECULES23040938.

[85] Wu D, Zhu L, Li Y, Zhang X, Xu S, Yang G, et al. Chitosan-based Colloidal Polyelectrolyte Complexes for Drug Delivery: A Review. Carbohydr Polym 2020;238. https://doi.org/10.1016/j.carbpol.2020.116126.

[86] Jin T, Liu T, Lam E, Moores A. Chitin and chitosan on the nanoscale. Nanoscale Horiz 2021;6:505–42. https://doi.org/10.1039/D0NH00696C.

[87] Ali A, Ahmed S. A review on chitosan and its nanocomposites in drug delivery. Int J Biol Macromol 2018;109:273–86. https://doi.org/10.1016/J.IJBIOMAC.2017.12.078.

[88] Abd El-Hack ME, El-Saadony MT, Shafi ME, Zabermawi NM, Arif M, Batiha GE, et al. Antimicrobial and antioxidant properties of chitosan and its derivatives and their applications: A review. Int J Biol Macromol 2020;164:2726–44. https://doi.org/10.1016/J.IJBIOMAC.2020.08.153.

[89] Pedro AS, Cabral-Albuquerque E, Ferreira D, Sarmento B. Chitosan: An option for development of essential oil delivery systems for oral cavity care? Carbohydr Polym 2009;76:501–8. https://doi.org/10.1016/J.CARBPOL.2008.12.016.

[90] Rizeq BR, Younes NN, Rasool K, Nasrallah GK. Synthesis, Bioapplications, and Toxicity Evaluation of Chitosan-Based Nanoparticles. International Journal of Molecular Sciences 2019, Vol 20, Page 5776 2019;20:5776. https://doi.org/10.3390/IJMS20225776.

[91] Grabovac V, Guggi D, Bernkop-Schnürch A. Comparison of the mucoadhesive properties of various polymers. Adv Drug Deliv Rev 2005;57:1713–23. https://doi.org/10.1016/J.ADDR.2005.07.006.

[92] Zhao D, Yu S, Sun B, Gao S, Guo S, Zhao K. Biomedical Applications of Chitosan and Its Derivative Nanoparticles. Polymers 2018, Vol 10, Page 462 2018;10:462. https://doi.org/10.3390/POLYM10040462.

[93] Nandi G, Hasnain MS, Nayak AK. Polysaccharide-based polyelectrolyte complex systems in drug delivery. Tailor-Made Polysaccharides in Drug Delivery 2023:177–210. https://doi.org/10.1016/B978-0-12-821286-8.00009-4.

[94] Kulkarni AD, Vanjari YH, Sancheti KH, Patel HM, Belgamwar VS, Surana SJ, et al. Polyelectrolyte complexes: mechanisms, critical experimental aspects, and applications. Https://DoiOrg/103109/2169140120151129624 2016;44:1615–25. https://doi.org/10.3109/21691401.2015.1129624.

[95] Lankalapalli S, Kolapalli VRM. Polyelectrolyte Complexes: A Review of their Applicability in Drug Delivery Technology. Indian J Pharm Sci 2009;71:481. https://doi.org/10.4103/0250-474X.58165.

[96] Kumar S, Kaur P, Bernela M, Rani R, Thakur R. Ketoconazole encapsulated in chitosan-gellan gum nanocomplexes exhibits prolonged antifungal activity. Int J Biol Macromol 2016;93:988–94. https://doi.org/10.1016/J.IJBIOMAC.2016.09.042.

[97] Costa ALR, de la Torre LG. Gellan gum nanoparticles in drug delivery. Micro- and Nanoengineered Gum-Based Biomaterials for Drug Delivery and Biomedical

Applications, Elsevier; 2022, p. 127–56. https://doi.org/10.1016/B978-0-323-90986-0.00009-1.

[98] Palumbo FS, Federico S, Pitarresi G, Fiorica C, Giammona G. Gellan gum-based delivery systems of therapeutic agents and cells. Carbohydr Polym 2020;229:115430. https://doi.org/10.1016/J.CARBPOL.2019.115430.

[99] Giavasis I, Harvey LM, McNeil B. Gellan gum. Crit Rev Biotechnol 2000;20:177–211. https://doi.org/10.1080/07388550008984169.

[100] Gehrcke M, de Bastos Brum T, da Rosa LS, Ilha BD, Soares FZM, Cruz L. Incorporation of nanocapsules into gellan gum films: A strategy to improve the stability and prolong the cutaneous release of silibinin. Materials Science and Engineering: C 2021;119:111624. https://doi.org/10.1016/J.MSEC.2020.111624.

[101] Cardoso VM de O, Brito NAP de, Ferreira NN, Boni FI, Ferreira LMB, Carvalho SG, et al. Design of mucoadhesive gellan gum and chitosan nanoparticles intended for colon-specific delivery of peptide drugs. Colloids Surf A Physicochem Eng Asp 2021;628. https://doi.org/10.1016/j.colsurfa.2021.127321.

[102] Picone CSF, Cunha RL. Chitosan-gellan electrostatic complexes: Influence of preparation conditions and surfactant presence. Carbohydr Polym 2013;94:695–703. https://doi.org/10.1016/j.carbpol.2013.01.092.

[103] Weidmann AE. Dihydroquercetin: More than just an impurity? Eur J Pharmacol 2012;684:19–26. https://doi.org/10.1016/J.EJPHAR.2012.03.035.

[104] Das A, Baidya R, Chakraborty T, Samanta AK, Roy S. Pharmacological basis and new insights of taxifolin: A comprehensive review. Biomedicine & Pharmacotherapy 2021;142:112004. https://doi.org/10.1016/J.BIOPHA.2021.112004.

[105] Sunil C, Xu B. An insight into the health-promoting effects of taxifolin (dihydroquercetin). Phytochemistry 2019;166:112066. https://doi.org/10.1016/J.PHYTOCHEM.2019.112066.

[106] Zhang HQ, Wang YJ, Yang GT, Gao Q Le, Tang MX. Taxifolin inhibits receptor activator of NF-κB ligand-induced osteoclastogenesis of human bone marrow-derived macrophages in vitro and prevents lipopolysaccharide-induced bone loss in Vivo. Pharmacology 2019;103:101–9. https://doi.org/10.1159/000495254.

[107] Artem'eva OA, Pereselkova DA, Fomichev YP. Dihydroquercetin, the bioactive substance, to be used against pathogenic microorganisms as an alternative to antibiotics. Sel'skokhozyaistvennaya Biologiya 2015;50:513–9. https://doi.org/10.15389/AGROBIOLOGY.2015.4.513ENG.

[108] Chen X, Huang J, Hu Z, Zhang Q, Li X, Huang D. Protective effects of dihydroquercetin on an APAP-induced acute liver injury mouse model. Int J Clin Exp Pathol 2017;10:10223–32.

[109] Shu Z, Yang Y, Yang L, Jiang H, Yu X, Wang Y. Cardioprotective effects of dihydroquercetin against ischemia reperfusion injury by inhibiting oxidative stress and endoplasmic reticulum stress-induced apoptosis via the PI3K/Akt pathway. Food Funct 2019;10:203–15. https://doi.org/10.1039/C8FO01256C.

[110] Li J, Hu L, Zhou T, Gong X, Jiang R, Li H, et al. Taxifolin inhibits breast cancer cells proliferation, migration and invasion by promoting mesenchymal to epithelial transition via β-catenin signaling 2019. https://doi.org/10.1016/j.lfs.2019.116617.

[111] Wang R, Zhu X, Wang Q, Li X, Wang E, Zhao Q, et al. The anti-tumor effect of taxifolin on lung cancer via suppressing stemness and epithelial-mesenchymal transition in vitro and oncogenesis in nude mice. Ann Transl Med 2020;8:590–590. https://doi.org/10.21037/ATM-20-3329.

[112] Razak S, Afsar T, Ullah A, Almajwal A, Alkholief M, Alshamsan A, et al. Taxifolin, a natural flavonoid interacts with cell cycle regulators causes cell cycle arrest and causes tumor regression by activating Wnt/ β-catenin signaling pathway n.d. https://doi.org/10.1186/s12885-018-4959-4.

[113] Nifant'ev EE, Koroteev MP, Kaziev GZ, Uminskii AA, Grachev AA, Men'Shov VM, et al. On the problem of identification of the dihydroquercetin flavonoid. Russ J Gen Chem 2006;76:161–3. https://doi.org/10.1134/S1070363206010324.

[114] Jomová K, Hudecova L, Lauro P, Simunkova M, Alwasel SH, Alhazza IM, et al. A switch between antioxidant and prooxidant properties of the phenolic compounds myricetin, morin, 3',4'-dihydroxyflavone, taxifolin and 4-hydroxy-coumarin in the presence of copper(II) ions: A spectroscopic, absorption titration and DNA damage study. Molecules 2019;24. https://doi.org/10.3390/MOLECULES24234335.

[115] Taldaev A, Terekhov RP, Selivanova IA, Pankov DI, Anurova MN, Markovina IY, et al. Modification of Taxifolin Properties by Spray Drying. Sci Pharm 2022;90. https://doi.org/10.3390/scipharm90040067.

[116] Ge Y, Zhang Y, He S, Nie F, Teng G, Gu N. Fluorescence modified chitosan-coated magnetic nanoparticles for high-efficient cellular imaging. Nanoscale Res Lett 2009;4:287–95. https://doi.org/10.1007/S11671-008-9239-9/FIGURES/11.

[117] Prabha S, Arya G, Chandra R, Ahmed B, Nimesh S. Effect of size on biological properties of nanoparticles employed in gene delivery.

Https://DoiOrg/103109/216914012014913054 2014;44:83–91. https://doi.org/10.3109/21691401.2014.913054.

[118] Danaei M, Dehghankhold M, Ataei S, Davarani FH, Javanmard R, Dokhani A, et al. pharmaceutics Impact of Particle Size and Polydispersity Index on the Clinical Applications of Lipidic Nanocarrier Systems 2018. https://doi.org/10.3390/pharmaceutics10020057.

[119] Leary JF, Endowed Professor of Nanomedicine S. "The Importance of Zeta Potential for Drug/Gene Delivery in Nanomedicine" 2011.

[120] Pandey YN, Papakonstantopoulos GJ, Doxastakis M. Polymer/nanoparticle interactions: Bridging the gap. Macromolecules 2013;46:5097–106. https://doi.org/10.1021/MA400444W/ASSET/IMAGES/MEDIUM/MA-2013-00444W_0007.GIF.

[121] Abyadeh M, Karimi Zarchi AA, Faramarzi MA, Amani A. Evaluation of Factors Affecting Size and Size Distribution of Chitosan-Electrosprayed Nanoparticles. Avicenna J Med Biotechnol 2017;9:126.

[122] Mirtajaddini SA, Najafi MF, Yazdi SAV, Oskuee RK. Preparation of Chitosan Nanoparticles as a Capable Carrier for Antigen Delivery and Antibody Production. Iran J Biotechnol 2021;19:e2871. https://doi.org/10.30498/IJB.2021.247747.2871.

[123] Li F, Chen Y, Liu S, Qi J, Wang W, Wang C, et al. Size-controlled fabrication of zein nano/microparticles by modified anti-solvent precipitation with/without sodium caseinate. Int J Nanomedicine 2017;12:8197–209. https://doi.org/10.2147/IJN.S143733.

[124] Rudyak VY, Krasnolutskii SL. Dependence of the viscosity of nanofluids on nanoparticle size and material. Phys Lett A 2014;378:1845–9. https://doi.org/10.1016/J.PHYSLETA.2014.04.060.

[125] Rodolfo C, Eusébio D, Ventura C, Nunes R, Florindo HF, Costa D, et al. Design of Experiments to Achieve an Efficient Chitosan-Based DNA Vaccine Delivery System. Pharmaceutics 2021, Vol 13, Page 1369 2021;13:1369. https://doi.org/10.3390/PHARMACEUTICS13091369.

[126] Batista-Silva J, Gomes D, Barroca-Ferreira J, Gallardo E, Sousa Â, Passarinha LA. Specific Six-Transmembrane Epithelial Antigen of the Prostate 1 Capture with Gellan Gum Microspheres: Design, Optimization and Integration. International Journal of Molecular Sciences 2023, Vol 24, Page 1949 2023;24:1949. https://doi.org/10.3390/IJMS24031949.

[127] Li MM, Peng RY, Wang WJ, Xu HX, Yin ZP, Chen JG, et al. Interaction with taxifolin reduces the digestibility of corn starch in vitro and in vivo. Journal of

Food Measurement and Characterization 2023. https://doi.org/10.1007/S11694-023-01930-8.

[128] Krysa M, Szymańska-Chargot M, Zdunek A. FT-IR and FT-Raman fingerprints of flavonoids – A review. Food Chem 2022;393:133430. https://doi.org/10.1016/J.FOODCHEM.2022.133430.

[129] Lim C, Hwang DS, Lee DW. Intermolecular interactions of chitosan: Degree of acetylation and molecular weight. Carbohydr Polym 2021;259:117782. https://doi.org/10.1016/J.CARBPOL.2021.117782.

[130] Patravale V, Dandekar P, Jain R. Characterization techniques for nanoparticulate carriers. Nanoparticulate Drug Delivery 2012:87–121. https://doi.org/10.1533/9781908818195.87.

[131] Chithrani BD, Ghazani AA, Chan WCW. Determining the size and shape dependence of gold nanoparticle uptake into mammalian cells. Nano Lett 2006;6:662–8. https://doi.org/10.1021/NL052396O.

[132] Jyothi NVN, Prasanna PM, Sakarkar SN, Prabha KS, Ramaiah PS, Srawan GY. Microencapsulation techniques, factors influencing encapsulation efficiency. Http://DxDoiOrg/103109/02652040903131301 2010;27:187–97. https://doi.org/10.3109/02652040903131301.

[133] Kim EJ, Choi JH, Yang HJ, Choi SS, Lee HK, Cho YC, et al. Comparison of high and low molecular weight chitosan as in-vitro boosting agent for photodynamic therapy against Helicobacter pylori using methylene blue and endoscopic light. Photodiagnosis Photodyn Ther 2019;26:111–5. https://doi.org/10.1016/J.PDPDT.2019.03.005.

[134] Yousefi M, Shadnoush M, Sohrabvandi S, Khorshidian N, Mortazavian AM. Encapsulation Systems for Delivery of Flavonoids: A Review 2021;11:13934–51. https://doi.org/10.33263/BRIAC116.1393413951.

[135] Hu Y, Zhang W, Ke Z, Li Y, Zhou Z. In vitro release and antioxidant activity of Satsuma mandarin (Citrus reticulata Blanco cv. unshiu) peel flavonoids encapsulated by pectin nanoparticles. Int J Food Sci Technol 2017;52:2362–73. https://doi.org/10.1111/IJFS.13520.

[136] Deepika MS, Thangam R, Sheena TS, Sasirekha R, Sivasubramanian S, Babu MD, et al. A novel rutin-fucoidan complex based phytotherapy for cervical cancer through achieving enhanced bioavailability and cancer cell apoptosis. Biomed Pharmacother 2019;109:1181–95. https://doi.org/10.1016/J.BIOPHA.2018.10.178.

[137] Rahimi S, Khoee S, Ghandi M. Preparation and characterization of rod-like chitosan–quinoline nanoparticles as pH-responsive nanocarriers for quercetin

delivery. Int J Biol Macromol 2019;128:279–89. https://doi.org/10.1016/J.IJBIOMAC.2019.01.137.